LAMS-2529

C.3



# LOS ALAMOS SCIENTIFIC LABORATORY

OF THE UNIVERSITY OF CALIFORNIA o LOS ALAMOS NEW MEXICO

## QUARTERLY STATUS REPORT OF THE LASL CONTROLLED THERMONUCLEAR RESEARCH PROGRAM FOR PERIOD ENDING FEBRUARY 20, 1961

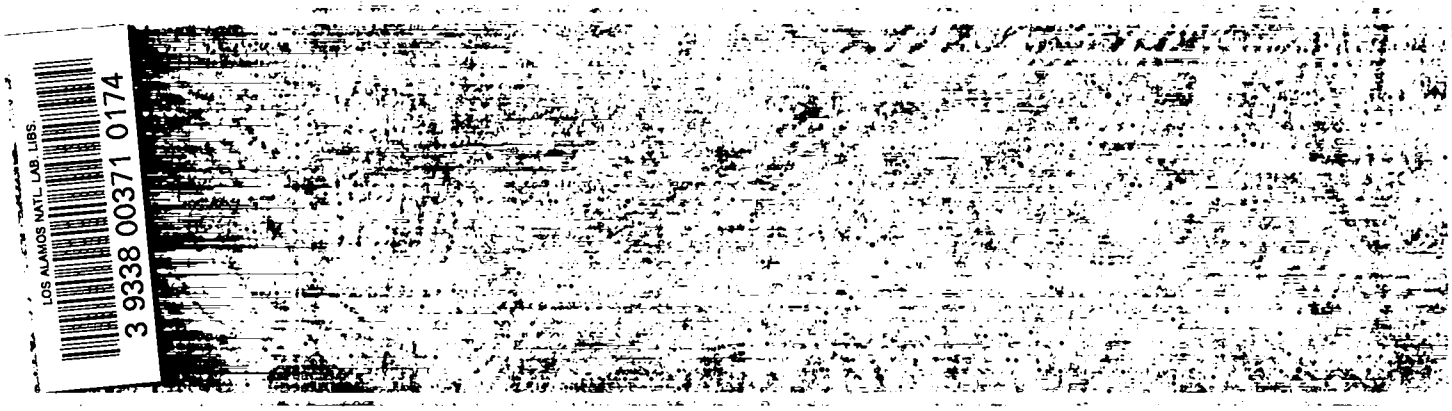

Printed in USA. Price $1.25. Available from the

Office of Technical Services
U. S. Department of Commerce
Washington 25, D. C.

LAMS-2529
CONTROLLED THERMONUCLEAR
PROCESSES
(TID-4500, 16th Ed.)

LOS ALAMOS SCIENTIFIC LABORATORY
OF THE UNIVERSITY OF CALIFORNIA LOS ALAMOS NEW MEXICO

REPORT COMPILED: March 1961
REPORT DISTRIBUTED: March 31, 1961

# QUARTERLY STATUS REPORT OF THE LASL CONTROLLED THERMONUCLEAR RESEARCH PROGRAM FOR PERIOD ENDING FEBRUARY 20, 1961

Prepared from material supplied by members of P Division


**Contract W-7405-ENG. 36 with the U. S. Atomic Energy Commission**

## SUMMARY

1. The half-scale caulked picket fence experiment is in operation. By varying the ratio of currents in the external and internal coils the magnetic field configuration can be changed from the conventional magnetic mirror field to two picket fence fields connected by a magnetic bridge. There does not seem to be any trapping of high-$\beta$ plasma in the magnetic mirror configuration while in the picket fence geometry there is trapping and containment of low-$\beta$ plasma between the line cusp and the axial cusp on the side away from the gun. The lifetime of trapped plasma in the caulked picket fence is not appreciably longer than that in the simple picket fence.

2. Time-resolved pressure distributions have been measured in the fast hydromagnetic gun. The electromagnetic valve on the plenum is found to open $\sim$ 150 $\mu$sec after the onset of the current signal to the valve and remain open $\sim$ 250 $\mu$sec. The gas pressure distributions show pressure peaks over the gas entrance holes and by $\sim$ 400 $\mu$sec the distribution is tending to become flat.

3. Preliminary data have been taken on Columbus S-5, a fast dynamic pinch experiment. The current sheet in the pinch is somewhat thicker than expected; at an initial electric field of $\sim$ 300 volts/cm, gas pressure of $\sim$ 75 microns of deuterium, the sheet is 13 mm thick and attains a velocity of $\sim 7 \times 10^6$ cm/sec.

4. Energy balance calculations have been made for several applied voltage discharges in Perhapsatron S-5 Zeus which indicate a negligible energy loss (within the accuracy of the measurements) for the first 20 $\mu$sec. Current density distributions show a current sheath starting at the wall and diffusing

inward, reaching the center of the discharge at ~ 5 μsec. Unfortunately, the quartz torus has broken for the second time. The failure was similar to the first one; a number of fine cracks developed about one of the weld joints.

5. The "tail" in the skew trapping experiment discussed in the preceding quarterly report has been found to be spurious. An extensive survey of input positions and angles was made for the symmetric coil configuration and no evidence of trapping for periods greater than 1 to 2 μsec was found. The experiment has been terminated.

6. A new idea for injecting and trapping energetic charged particles in magnetic mirror geometries has been proposed by R. C. Wingerson (MIT). The magnetic field between the mirror is weakly modulated by a magnetic field which is both perpendicular to the main field axis and which rotates spatially about the axis. If a charged particle is injected parallel to the axis a resonance condition exists between (a) the longitudinal velocity of the particle, (b) the strength of the main magnetic field, and (c) the period of the modulating magnetic field, at which longitudinal energy is transferred into perpendicular energy. If on subsequent traversals of the particle through the modulation field perpendicular energy is not transferred rapidly back into longitudinal energy, particles may be trapped between the mirrors for times of interest in Project Sherwood. Theoretical calculations have been made of the resonance condition for a simplified model and an electron experiment has been set up. The resonance condition has been verified with three quarters of the initial injected energy (2 kev) transferred into perpendicular energy.

7. In the experiment on the scattering of microwaves by ionized gases the dynamics of the plasma medium have been detected both by incoherent scattering out of the main beam and phase modulation of the transmitted beam. A resonance in the intensity of the incoherent scattered beam has been found which depends upon gas pressure and electron density, n. The resonance

has been studied with six different gases and shows (with the exception of helium where no resonance has yet been found) that at resonance n/M (M = atomic mass) is approximately a constant.

8. Small azimuthal asymmetries in the axial magnetic have been found to reduce the neutron yield in the Orthogonal Pinch experiment by a factor of as much as three. It is felt that small asymmetries affect adversely not only the initial stage of ionization but the uniform detachment of the current layer from the inner surface of the glass wall. The dependence of neutron yield on voltage has been extended to 22 kv by overvoltaging the capacitors. The neutron yield has been found to increase by a factor $\sim 2$ per kilovolt increase in voltage (15 to 18 kv) and by only $\sim 1.5$ per kilovolt at higher voltages (18 to 22 kv). At the higher voltages there is evidence of enhanced impurity contamination, asymmetric neutron pulse shapes, and visible light. These results suggest that the optimum energy density or applied voltage is being reached.

9. The effects of irradiation on the four-electrode Marx gap have been studied by applying a slowly rising trigger pulse to the probe of the center electrode. It was found that the gap could be fired at voltages from 2 to 30 kv. Irradiation of the gap very greatly reduces the jitter time, and with a steep trigger pulse the jitter in firing may be kept below 0.1 μsec.

10. In connection with the Scylla experiment, the reflectivity of the beryl crystal of the soft x-ray spectrometer has been measured. In addition the shape and absolute magnitude of the continuum spectrum from Scylla I have been measured. The results show the electron temperature to be $345 \pm 30$ ev with pure deuterium gas and the intensity to be largely due to recombination radiation from highly stripped impurity ions in the discharge.

11. Scylla III (30 Tobe capacitors) with the standard Scylla I coil has produced $10^8$ neutrons during a discharge. This is within a factor of two of the yield to be expected on the basis of an extrapolation of the Scylla I

yield, assuming magnetic compression heating. The corresponding ion temperature is about 2.1 kev.

12. The new plasma gun is producing what appears to be a dense, highly energetic plasma stream. An experiment is being performed to study the guiding of the stream by, and piercing by the stream of, a longitudinal magnetic field. This is preliminary to an experiment, now under construction, in which two such plasma streams will be collided inside a longitudinal magnetic field. If there is appreciable conversion of the translational energies of the streams to random energy this may provide an excellent injection method for plasma reactors.

13. Construction of the E X B accelerator is nearly complete except for the coil which furnishes the transverse magnetic field. The latter is being redesigned.

14. A total of 16 of the 42 shelves of the Zeus capacitor bank have been test fired at full voltage. Assembly and testing of one shelf of the Zeus bank using a new low inductance cabling scheme has been completed. The results show that the inductance of the new system is one half that of the previous design and has other mechanical and electrical advantages. The new inductance value is 0.030 μh for one shelf (1/7 megajoule).

15. Development work on the fast, parallel-plate capacitor has resulted in improved designs which are expected to permit extension of the working voltage to 50 kv. Difficulties with the tab construction appear to have been eliminated and test samples of a design to overcome edge failures are being prepared.

## A. CAULKED PICKET FENCE

The half-scale model of the caulked picket fence apparatus has been operated with three different magnetic field configurations, viz., a caulked picket fence, a simple picket fence, and a mirror machine. To transform from one machine to another, all that is necessary is to change the relative currents in the field-producing coils. The maximum field in the machine for any of these geometries was ~ 400 gauss.

The injected deuterium plasma had sufficient energy density and electron density to pierce the 400-gauss field as a $\beta = 1$ plasma. Typical injection pulses lasted 5 μsec and contained ions with energies between 50 ev and 1 kev (the average being ~ 300 ev). The total amount of plasma entering the machine was 5 to 10 joules.

Magnetic probe studies lead to the following conclusions:

1) There does not seem to be any trapping of a high-$\beta$ plasma in the mirror machine.

2) Trapping and containment with 30 to 50-μsec lifetimes is observed in both the picket fence and caulked picket fence geometries.

3) The region of trapped plasma is very asymmetric around the zero in the magnetic field. Apparently, the plasma and field are sufficiently intermixed so that particles are reflected between the line cusp and the point cusp on the side away from the gun. There is not an appreciable amount of plasma trapped in the region between the input cusp and line cusp. The plasma observed in this region in an earlier experiment was probably due to wall interaction; a trapped plasma may be produced in this region in the present machine by simply adding "fake" walls close to the region of interest.

4) The lifetime of the plasma in the caulked picket fence is not appreciably longer than that in the simple picket fence.

The gun has been tuned up to inject helium in a pulse similar to the deuterium injection pulse. The purpose of this is to study the Doppler

broading of the HeII 4686 line as a function of time after injection. Background light from the gun has thus far prevented the measurement before 50 μsec after firing the gun. At 50 μsec, preliminary results indicate an ion energy of 70 ev and (combined with probe results) a density of $\sim 10^{13}$ ions/$cm^3$.

## B. HYDROMAGNETIC GUN RESEARCH

A test facility to be used for the study of the properties of hydromagnetic guns has been assembled. The principal parts are an expansion chamber 1 meter long and 1 meter in diameter, with a 70-cm long view port along the one side, and a plasma gun mounted at one end. The initial work has been conducted on the short, high-speed gun described in LAMS-2444 and LAMS-2464.

The first series of experiments was aimed toward the development of an electromagnetic,fast-acting gas valve. For this a 2-in. diameter valve was chosen using a single-turn drive coil to deflect the periphery of a 1.5-in. diameter Be-Cu diaphram (spring loaded) and unseat it from a Neoprene O-ring. This allows deuterium gas to escape from a $\sim 0.4$ $cm^3$ plenum through a series of holes into the region between electrodes. Time-resolved pressure distributions of the gas pulse have been measured at various positions along the gun using an open CK5702 subminature pentode as a fast-ion gage probe. This gage was statically calibrated against a VG-1A ion gage and is capable of detecting a pressure change of $\sim 3 \times 10^{-5}$ mm of Hg when used with a 50 K plate load resistor in a cathode follower circuit.

The experimental data show very good reproducibility in time and amount of gas released; however, the valve requires approximately 150 μsec after onset of current in the drive coil ($t = 0$) to open, and allows gas to enter up to $\sim 400$ μsec after $t = 0$. The amount of gas that enters is a function of the condenser voltage on the drive coil, e.g., $\sim 50\%$ of the gas in the plenum enters with 28 μf charged to 11 kv. Preliminary experiments using the plasma gun and the new fast gas valve described

above indicate operation very similar to that previously described for this gun. Measurements of the plasma density and velocity distribution have been started using a small ion collector probe, but diagnostic techniques must be improved before a systematic study of other gun geometries and gun parameters can be initiated.

## C. COLUMBUS S-5

The Columbus S-5 fast dynamic pinch apparatus was assembled and de-bugged, and some data were taken with electric and magnetic probes.

Preliminary results indicate that the current sheet of the pinch is somewhat thicker than had been expected. At an initial electric field of about 300 v/cm, and a pressure of 75 microns of deuterium, the sheet is about 13 mm thick, and attains a radial velocity of about $7 \times 10^6$ cm/sec. The electric field normal to the sheet apparently is adequate to stop deuterons entering the current sheet.

## D. PERHAPSATRON S-5 ZEUS

Fracture of the quartz torus liner has again stopped experimental work on the Perhapsatron S-5 Zeus (PS-5Z) machine. Breakage occurred with the system operating at 15 kv per quadrant, 2000 gauss stabilizing field, and 400 μ Hg deuterium gas pressure. The system had been operated successfully for many discharges (> 100) at these voltages but at pressures of 1 μ or less. A possible cause of the fracture was an electrical breakdown through the observation port to the grounded magnetic field probe inserted there. The higher operating pressure possibly facilitated the breakdown. An unbalance of discharge current in this quadrant would produce magnetic forces which may have ruptured the quartz torus. The break occurred at a weld in the quartz as in the previous case.

Some magnetic field probe data were obtained prior to the failure. A 21-coil probe was used to determine the field distribution simultaneously at a number of radial points within the discharge. The effects of varying

voltage, stabilizing field, and gas pressure on the sheath behavior, discharge stability, current distribution, and energy losses were observed. The failure of the system occurred, however, before this series of measurements was completed.

Energy balance calculations using the available data of the current, voltage, and probe measurements show negligible energy loss, within the accuracy of measurements, for the first ~ 20 μsec of the discharge. Typical results are shown in Figs. 1 and 2; Fig. 1 shows the energy delivered to the torus from the Zeus bank and the loss in the external circuit. Approximately 70 percent of the available energy ($\int V_g I_g dt$) is delivered to the torus. The distribution of this energy in the discharge is given in Fig. 2. Most of the energy goes into $B_\theta$ and $B_Z$ magnetic fields for the first 20 μsec, and only a small proportion, as indicated, into the plasma itself. The relative magnitude of this useful energy (for heating the plasma) is so small that experimental error makes it indeterminate. But after about 20 μsec, the magnetic energy curve dips abruptly away from the input energy ($\int V_g I_g dt$) curve indicating the onset of a radical energy loss. The cause of this loss effect has not been determined, but the onset time is approximately coincident with the abrupt decay of the neutron pulse and the onset of intense impurity light from the discharge.

Current density distributions have been determined for operating voltages ranging from 15 to 7.5 kv per quadrant. Results show a current sheath starting at the wall and diffusing inward to the center of the tube in ~ 5 μsec. The current channel at maximum current occupies half the tube diameter, decreasing slowly with voltage and current.

Probe traces show the results are not reproducible and a small scale flutter develops after ~ 4 μsec. But it is not apparent that these residual instabilities are immediately harmful in themselves since there are no large energy losses until ~ 20 μsec. However, a smaller energy loss comparable with the Joule energy in plasma heating may have occurred since these were relatively small and undetermined within the accuracy of measurement.

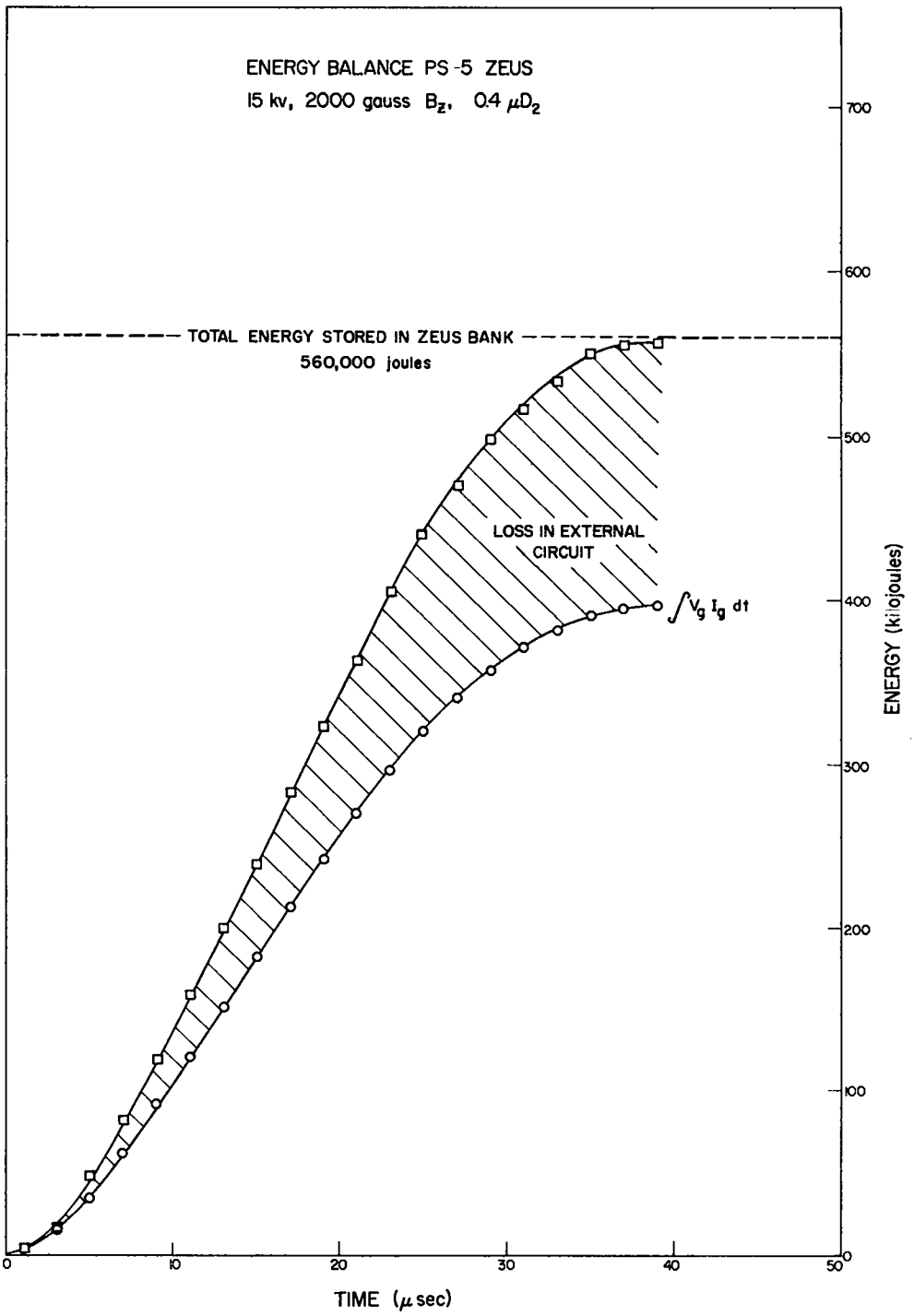


Fig. 1. Energy delivered from Zeus bank and loss in external circuit of PS-5Z.

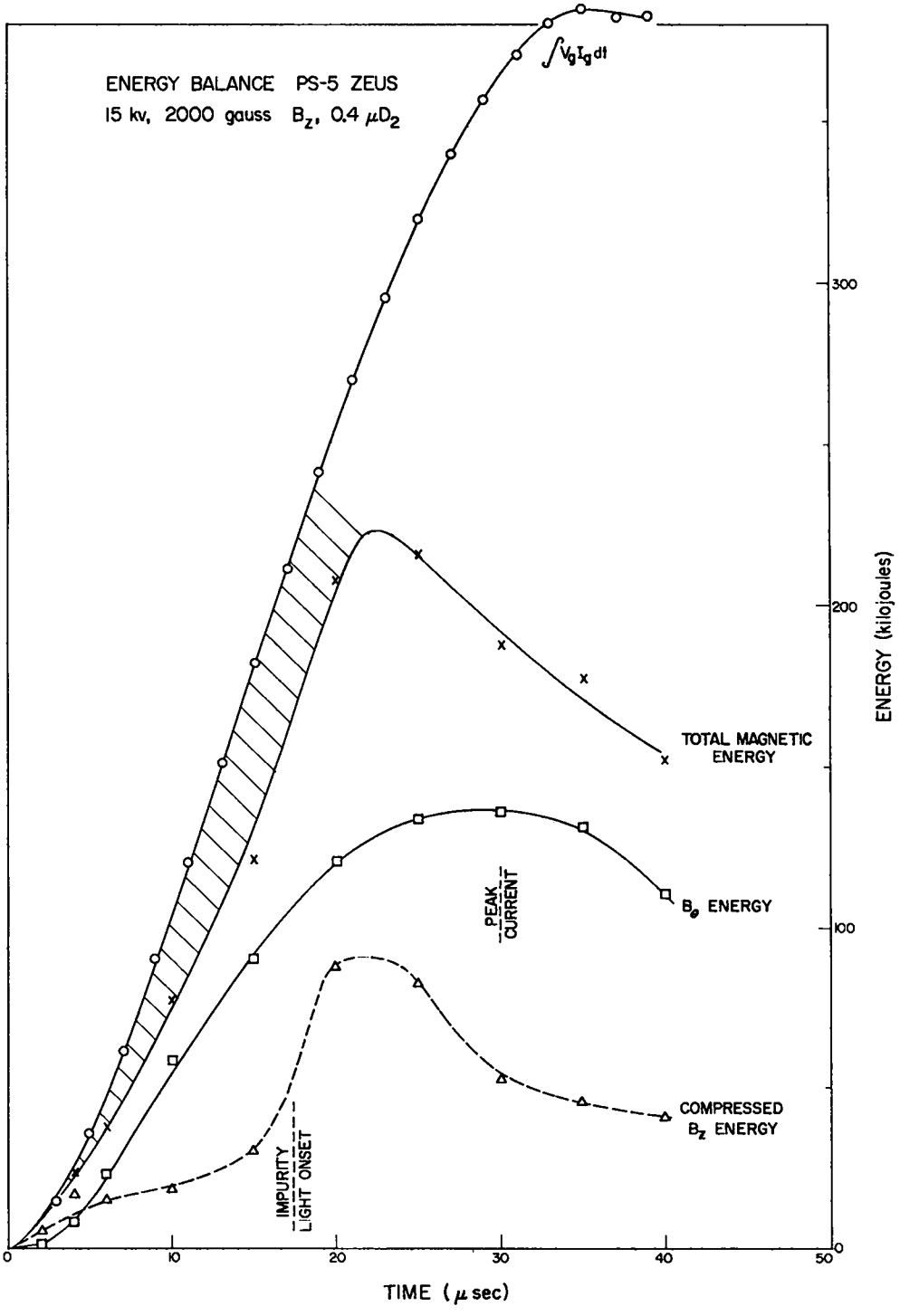


Fig. 2. Distribution of energy in PS-5Z

The PS-5Z program has been stopped for the present. The use of a ceramic-lined stainless steel torus as a substitute for the quartz system is being considered if the Perhapsatron work is resumed.

## E. SKEW TRAPPING

The 100-μsec tail discussed in the last quarterly report (LAMS-2488, p. 13) has been traced to an insulating surface accumulating charge during the beam pulse. When this surface is removed from the apparatus, the signal returns to normal. With the equipment behaving correctly, a complete survey of input positions and angles was made for the symmetric magnet configuration. This survey included approximately 1000 positions, and showed no evidence of trapping for periods greater than 1 to 2 μsec. After these negative results were obtained the experiment was terminated.

## F. RESONANCE HELIX TRAPPING EXPERIMENT

In the method proposed by Fedorchenko, et al., and by Sinelnikov, et al., in the U.S.S.R.,for introducing fast ions into a magnetic mirror geometry, auxiliary modulating coils locally modify the main magnetic field and off the axis produce magnetic fields perpendicular to the axis. A charged particle injected off the axis will experience alternately inward and outward radial magnetic fields which will deflect the particle first in one direction and then in another. By proper spacing of the modulating coils a resonance condition is attained and a significant fraction of the initial longitudinal energy may be directed into transverse energy and the particle trapped between the mirrors. If containment is to be successful, the probability of the reverse process must be small. Electron beam experiments show that electrons are trapped by this method.

A modification of the foregoing scheme has been proposed by R.C. Wingersen at M.I.T. in which the perturbing field is always perpendicular both to the axis and the motion of the particle, i.e., rotates in resonance with the orbiting particle. (Such a field may be formed by a helix of

variable pitch whose axis is coincident with the axis of the main field). The pitch of this rotating field must satisfy the resonant condition that the distance between adjacent turns is determined by the longitudinal velocity of the particle between these turns and as more of the longitudinal energy is directed into transverse energy the distance between turns must decrease. Using electrons, Wingerson has shown that (1) longitudinal energy is directed into transverse energy, (2) the resonance condition exists, and (3) electrons emerging from the modulating field are reflected by a magnetic mirror.

In considering the probability of reversal of the energy transfer, it should be noted that the helix has a sense of rotation (clockwise or counterclockwise) and a particle whose sense of rotation in the main field is constant finds upon returning to the helix that its motion will not now fit in with the "threads" of the helix but will cross-thread (as turning a left-handed nut on a right-handed screw). The motion of the particle is now not in resonance with the perturbing field and the transfer of energy into the longitudinal direction will be considerably reduced from the resonance case.

In view of the negative results of the Skew Trapping Experiment and the decision to terminate it, an investigation has been initiated of the Wingerson trapping scheme.

An electron analogue experiment is being carried out to determine the possibility of altering the magnetic moment of a particle injected axially in a magnetic mirror machine by means of a small perturbing magnetic field in the central region between the mirrors. The perturbing field rotates in space in phase with the Larmor motion of the particle. For the experiment, a 2-kev electron beam was directed axially into a mirror machine whose central magnetic field has a value of 100 gauss. The parameters determining resonance are then $\omega_c = eB/mc = 1.75 \times 10^9$ radians/sec, initial velocity $v_o = 2.7 \times 10^9$ cm/sec, and the initial spatial period ($L_o$) of the field perturbation as determined by the

resonance condition is $L_o = 2\pi v_o/\omega_c = 9.7$ cm. The Larmor radius of a 2-kev electron in a 100-gauss field is 1.5 cm.

A schematic diagram of the apparatus is shown in Fig. 3. The main axial magnetic field was produced in a large air-core solenoid of 20 in. bore and length ~ 2 meters. It provides a 100-gauss field with ease using a 7.5 kva full wave silicone rectifier power source, and ~ 20 amp current through the magnet. The mirror fields are produced with small insert coils at both ends of the large solenoid. These coils supply fields up to 1000 gauss, providing a variable mirror ratio up to 10. A current of 25 amp in these coils gave a mirror ratio of 2.

The coil producing the field perturbation was made in the form of a four-wire helix whose pitch, L(z), decreased as the cosine of the distance down the tube, i.e.,

$$L(z) = L_o \cos \frac{z\pi}{100} .$$

The total helix length was 50 cm. A photograph of the completed coil is shown in Fig. 4.

The perturbing field $B_r$ rotates with a period which varies along the helix. On the axis, the longitudinal field $B_z$, from the helix is zero. Off axis, the $B_z$ field has the same period as the helix. For the conditions of the experiment($L_o$ = 10 cm, coil diameter = 11 cm), a current of ~ 150 amp produces a perturbation in the front ($L_o$ end) of the helix of ~ 4 to 6 gauss. This perturbation drops off down the coil and is negligible after L(z) ~ 4 cm or z ~ 40 cm. If L is proportional to cos z, as postulated above,then $|B_r|$ also varies as cos z for the resonance condition to be satisfied through the full length of the helix. This is true to a fair approximation in this helix down to L(z) $\approx$ 5 cm. The magnitude of the perturbing field required for the particle to stay in resonance for the length of the helix is

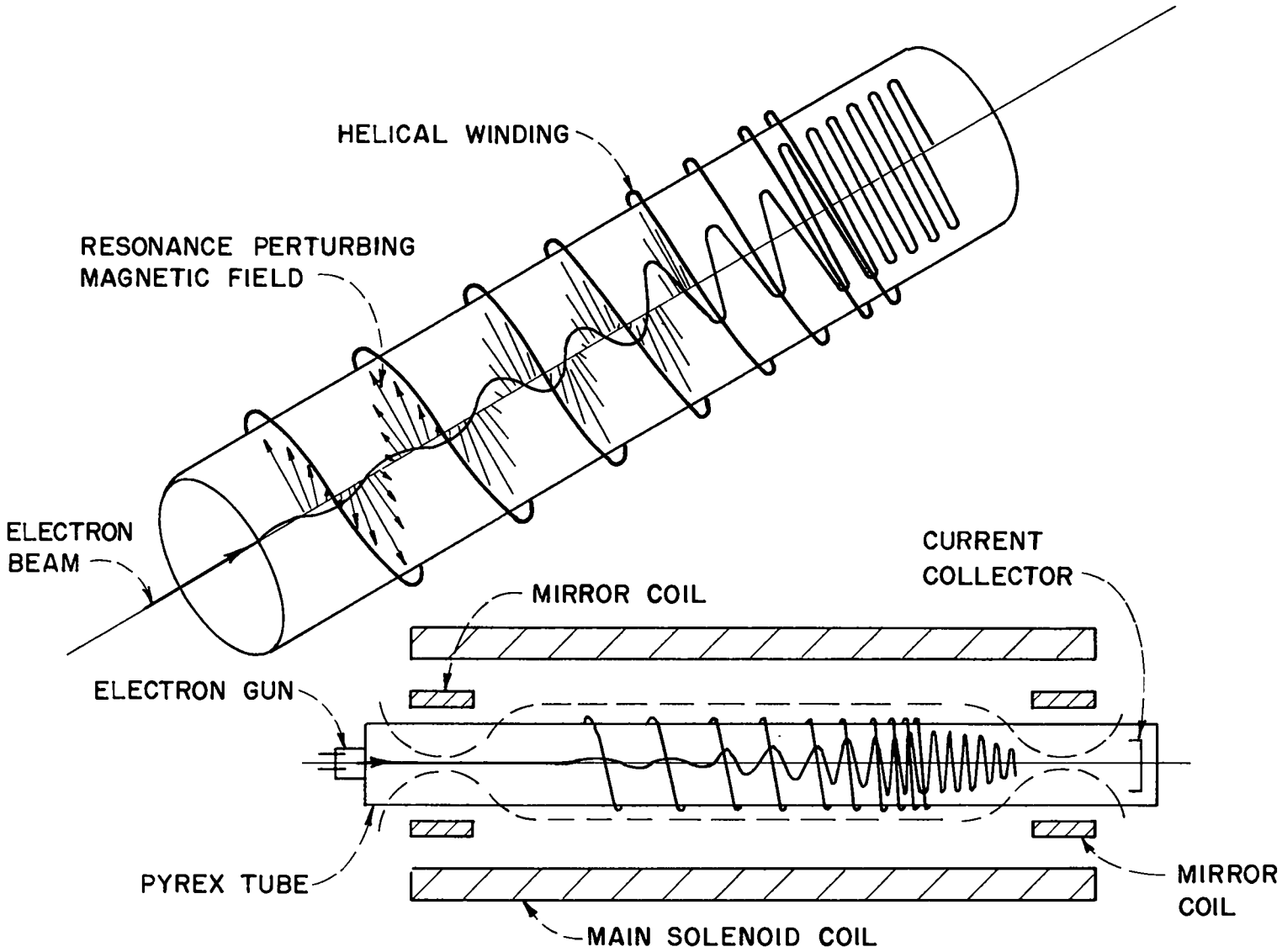


Fig. 3. Schematic of Resonance Helix Trapping Experiment

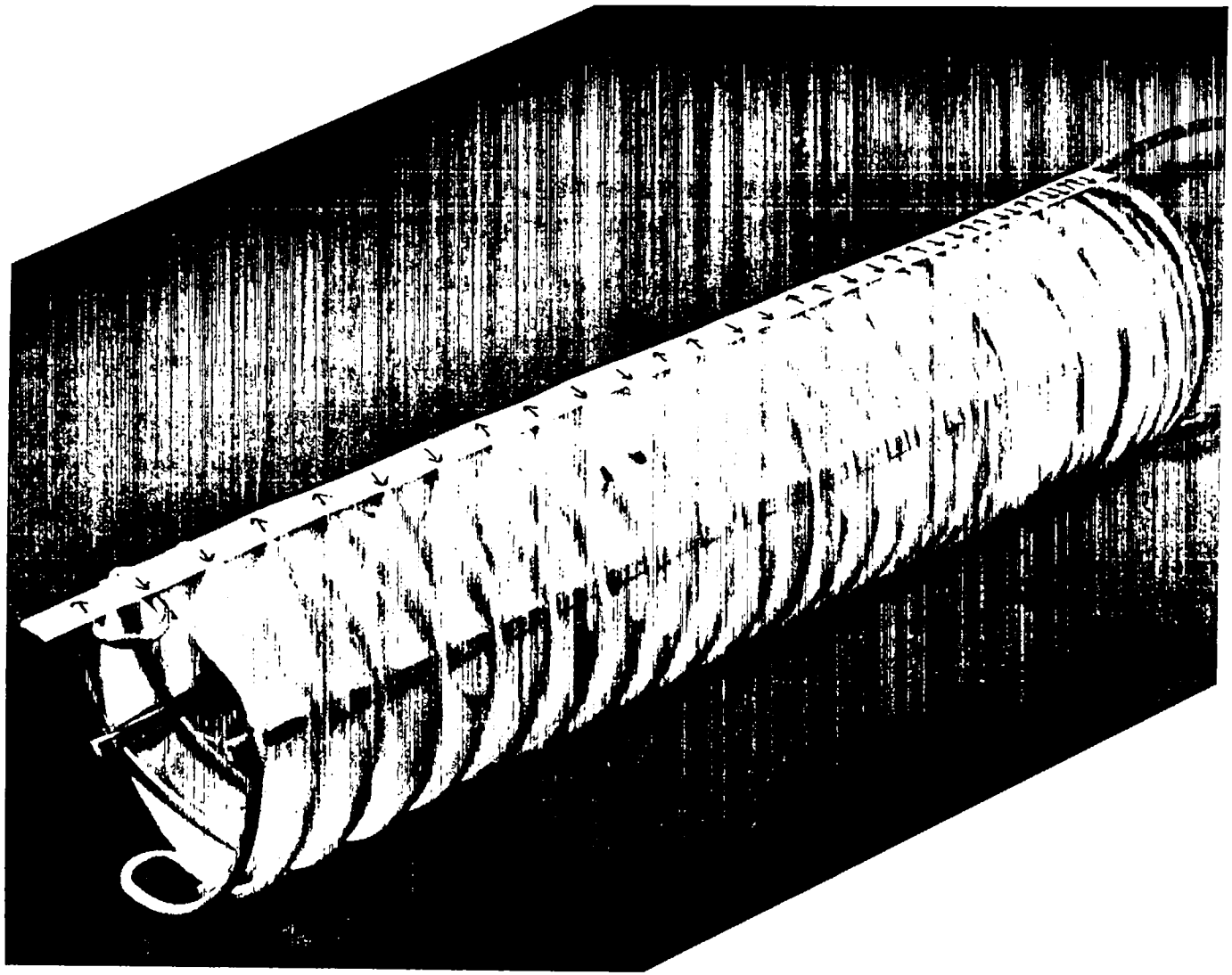

Fig. 4. Resonance Helix Trapping coil

$$\frac{e\, B_r(L_o)}{m\, c} \times \frac{2L(\text{helix})}{\pi} = v_o ,$$

where

$L(\text{helix})$ = length of helix = 50 cm

$B_r(L_o)$ = $B_r$ at the entrance to the helix

$v_o$ = initial velocity of injected particle.

Then $B_r(L_o) = 4.85$ gauss is required for the resonance parameters given above.

The electron gun for the experiment consists simply of a hot tantalum filament situated ~ 1/4 in. from a brass anode. A hole in the anode and the filament are aligned along a magnetic field line so the electrons are constrained to move in the axial direction. A series of collimators extend from the gun in the direction of the beam. The gun will provide electron currents up to 10 mamp. Beam blowup has not been investigated at full current, but at 1 mamp output no appreciable beam spreading is observed over the 2 meter length of the apparatus. The electron energy is variable from 0 to 3 kev.

The vacuum chamber consists of a 4-in. o.d., 1/4-in. wall Pyrex tube which is aligned carefully with the mirror coils and the main solenoid. The helix slips over the glass and is supported by it. A stainless steel wire mesh is inserted within the glass tube to provide an electrical ground around the containment region. The base pressure attainable in the containment region is ~ $10^{-3}$ $\mu$ Hg.

Two types of experiments have been performed with this apparatus: (1) visual observations with a glass plate coated with a scintillating material and aluminized to make it conducting, and (2) a current collecting cap with retarding grids to measure the current transmitted down the length of the tube and the energy distribution of the electron beam parallel to the magnetic field.

It is observed with the scintillating plate that the beam spot rotates about the centerline of the apparatus in a spiral of increasing radius as z is increased in phase with the rotation of the perturbing magnetic field for the following conditions: $B_{zo}$ = 100 gauss, E = 2 kev, $I_{helix}$ = 140 amp. These parameters correspond quite closely to the conditions predicted by the resonance equation. At the exit of the helix it is observed that $v_{11} = 1/2\ v_{11_o}$, or that three fourths of the original parallel energy has been converted into the perpendicular direction.

With $B_{zo}$ reversed, the electron rotates in a direction opposite to the rotation of the helix perturbation magnetic field. No resonant phenomenon then exists, and no measurable energy is transferred from the axial to the transverse direction. This is to be expected, for the Larmor motion is not in phase with the perturbing field as is required for the resonance effect. There should thus not be a serious loss in transverse energy of the particles as they pass back through the helical perturbation field after reflection by the magnetic mirror.

The resonance phenomena can also be observed by measuring the current transmitted through a mirror as a function of incident energy, helix current, and mirror ratio. Figure 5 shows the current transmitted through the far mirror (the mirror near the source is not activated) as a function of electron energy and helix current for a mirror ratio of 2. At approximately 130-amp helix current, the beam is completely reflected from the mirror for a small range of energy (~ 20% in energy or ~ 10% in velocity). Over this range of velocity the resonance condition $L_o = 2\pi v_{11}/\omega_c$ is satisfied and the magnitude of the perturbing field is such that at least half the initial energy is converted into the perpendicular direction. With this proportion of transverse energy, the electrons are reflected by the magnetic mirror (for mirror ratio $\geq$ 2) and the current to the collector falls almost to zero.

With both mirrors activated, it is observed that for the resonance conditions described above the whole tube between the mirrors glows with a

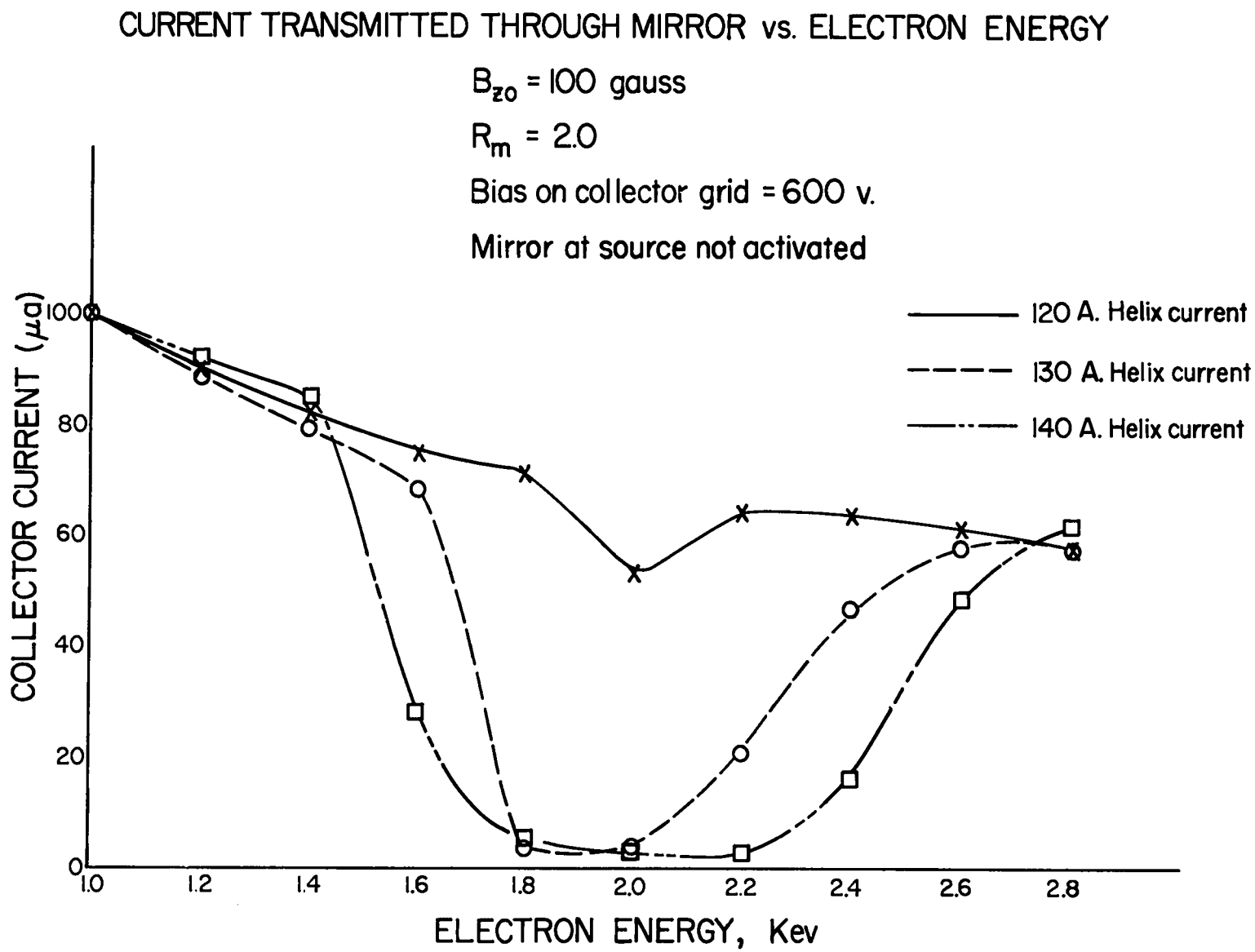


Fig. 5. Current transmitted as function of electron current

discharge ~ 4 cm in radius. This glow disappears when (a) an obstruction is placed in the mirror region, (b) the helix is run below 120 amp or above 180 amp or (c) the mirror ratio is lowered below ~ 1.7. With the scintillating plate placed just outside the peak of the mirror field, it is observed that as the helix current is increased the electron spot is transformed into a circle, and when the glow appears the circle on the scintillator disappears and a uniform illumination ~ 1.25 cm in diameter is seen on the scintillator. The diameter of this glow can be reduced by raising the mirror ratio, but as the mirror ratio is increased to ~ 6 the glow inside the tube is enhanced. The light emitted from the volume of the tube is clearly visible at 1 mamp input current and $p_o \sim 2\text{-}3 \times 10^{-6}$ mm Hg, conditions where no beam is visible when the machine is operated off resonance. The distribution of energy parallel to the magnetic field lines has been measured with a biased grid detector for the case where only one mirror is activated, and for the condition where both mirrors are connected and the glow is observed. These measurements, while only qualitative, show a wide distribution in energy for the case in which there are trapped particles, but a very narrow distribution in energy for the case where only one mirror is in use.

These measurements are preliminary, but they do indicate some confinement of electrons injected from outside the mirror system. Confinement times and energy distributions of particles emerging from the mirrors are in the process of being measured more carefully.

In addition to the experimental studies, calculations have been made for the case of a constant perturbing magnetic field superimposed on a constant field in the z direction, of strength $B_o$, such that a charged particle moving initially in the z-direction with a given velocity v will have its longitudinal motion changed into transverse motion in an essentially irreversible manner.

For certain simple forms of the perturbation, $\delta(z)$, of the magnetic field as a function of z-coordinate of a point in the particle trajectory,

analytical solutions of the problem are possible. One such form is

$$\delta(z) = \alpha \cos \alpha z,$$

for which the polar angle, $\theta$, i.e., the angle between the z-direction and the particle velocity, is given by

$$\theta = \alpha z,$$

and the azimuthal angle, $\phi$, is

$$\phi = -\frac{1}{\alpha} \log \tan \left(\frac{\pi}{4} + \frac{\alpha z}{2}\right).$$

The perturbing magnetic field at the particle trajectory then has the magnitude $\alpha \cos \alpha z$, and the direction

$$\theta = 0 \quad \text{and} \quad \phi = \frac{\pi}{2} - \frac{1}{\alpha} \log \tan \left(\frac{\pi}{4} + \frac{\alpha z}{2}\right).$$

The particle orbit has been computed by means of an IBM-704 program with $\alpha = 0.025$. In the forward direction, 95% of the kinetic energy of the particle was changed from longitudinal to transverse energy in about 13 turns. Then the z-component of the velocity was reversed and the particle carried back to $z = 0$. The maximum change in transverse energy moving in the reverse direction was only 0.8% of the total energy.

## G. SCATTERING OF MICROWAVES BY IONIZED GASES

Work has been under way for some time (see LAMS-2444, 2464, 2488) to determine the characteristics of microwaves scattered incoherently by an ionized gas. The experimental arrangements developed for this purpose are depicted schematically in Figs. 6 to 10.

A 200-watt CW (Litton) magnetron (Fig. 6), mechanically tuneable from 2300 to 3500 Mc/sec, provides the primary power which is beamed at a Pyrex scattering chamber filled with a partially ionized gas. Purity of spectrum above the magnetron carrier is achieved by passing the primary power through a five-section, low-pass filter whose cut-off frequency

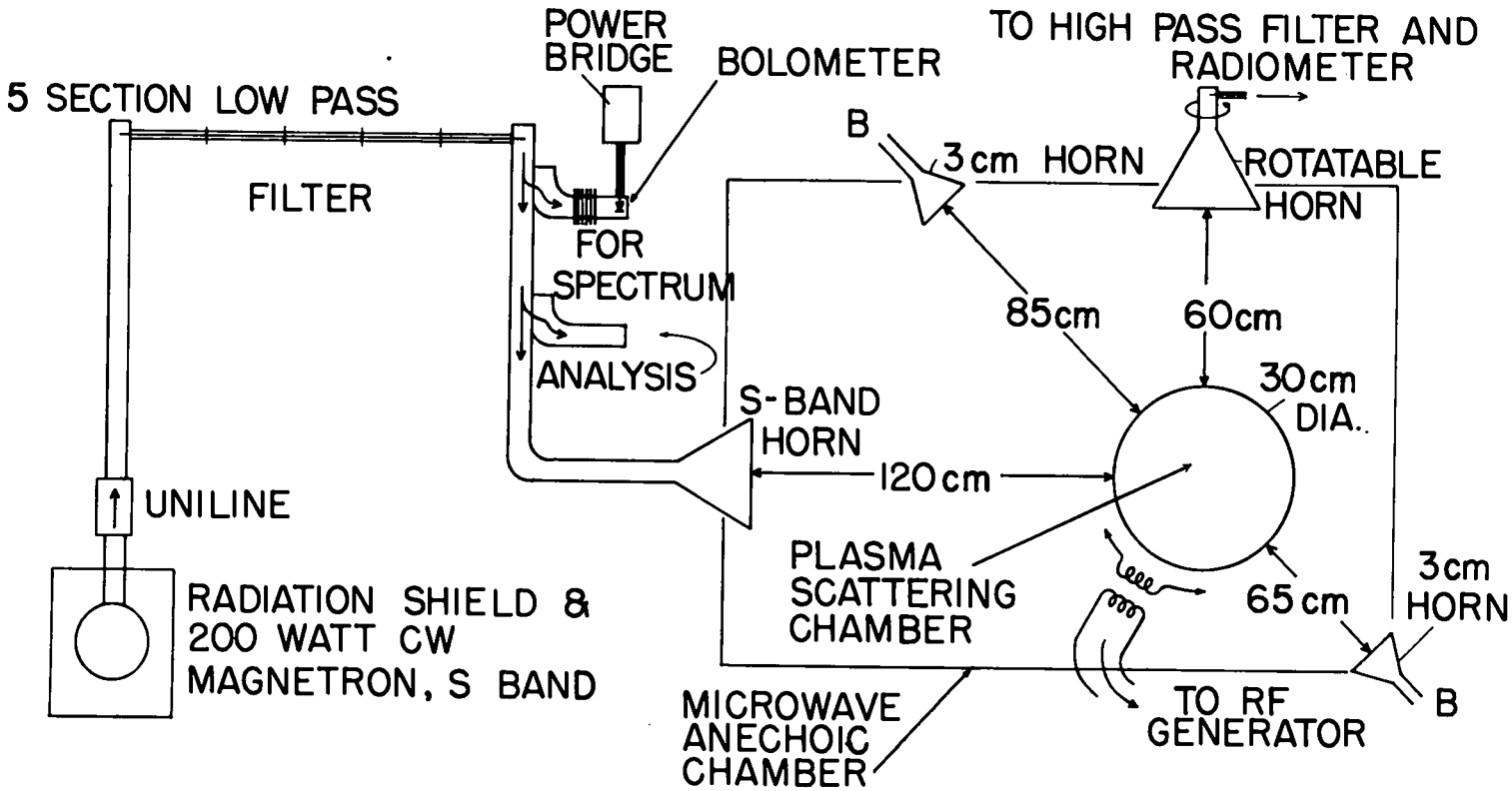


Fig. 6. Schematic of microwave scattering apparatus

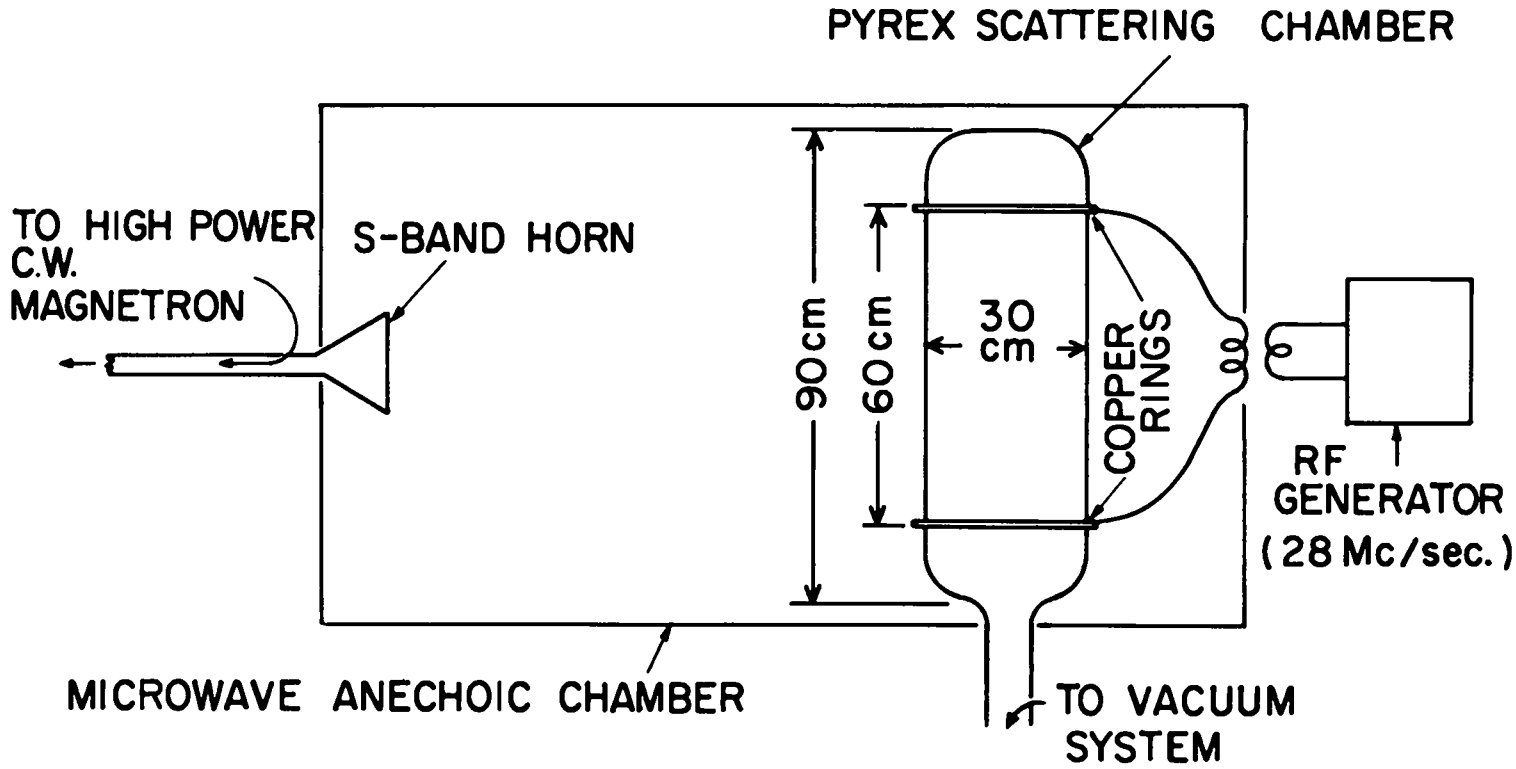


Fig. 7. Schematic of microwave scattering apparatus

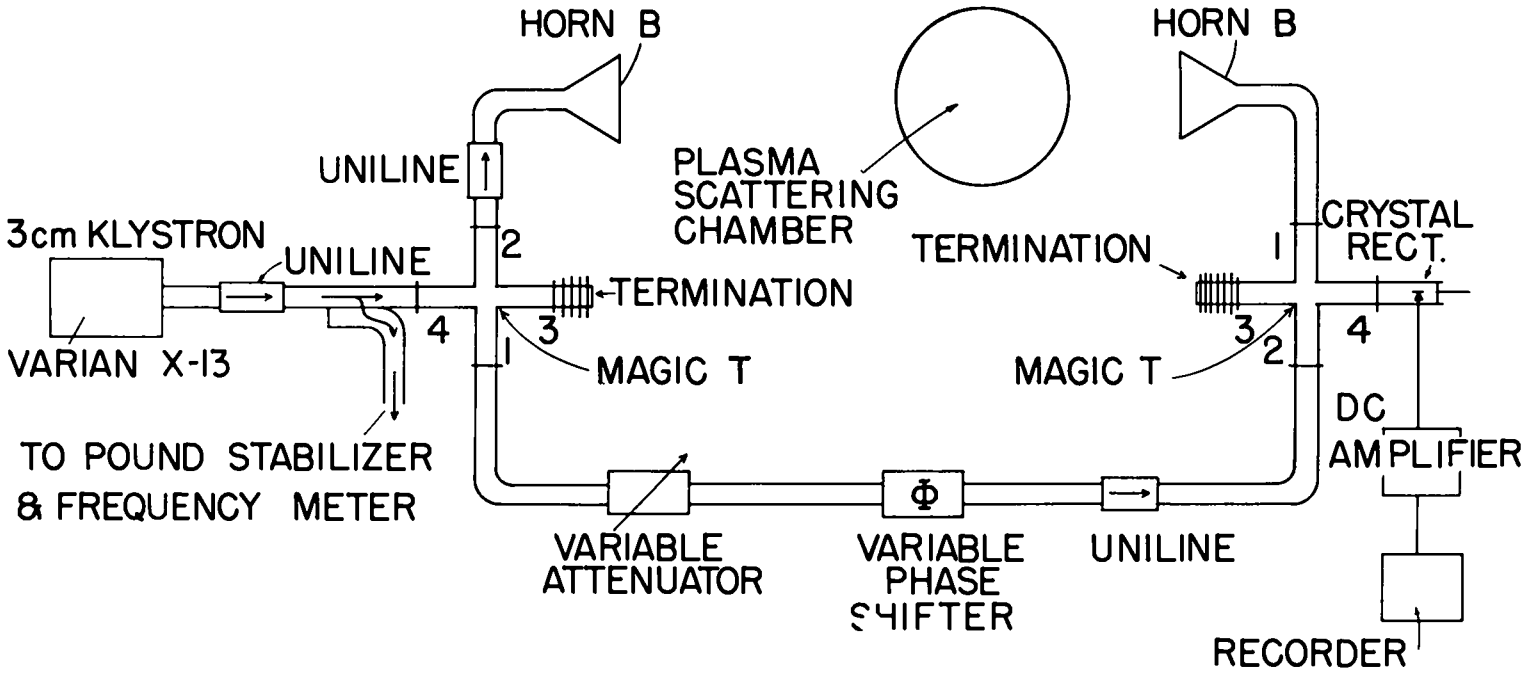


Fig. 8. Schematic of microwave scattering apparatus

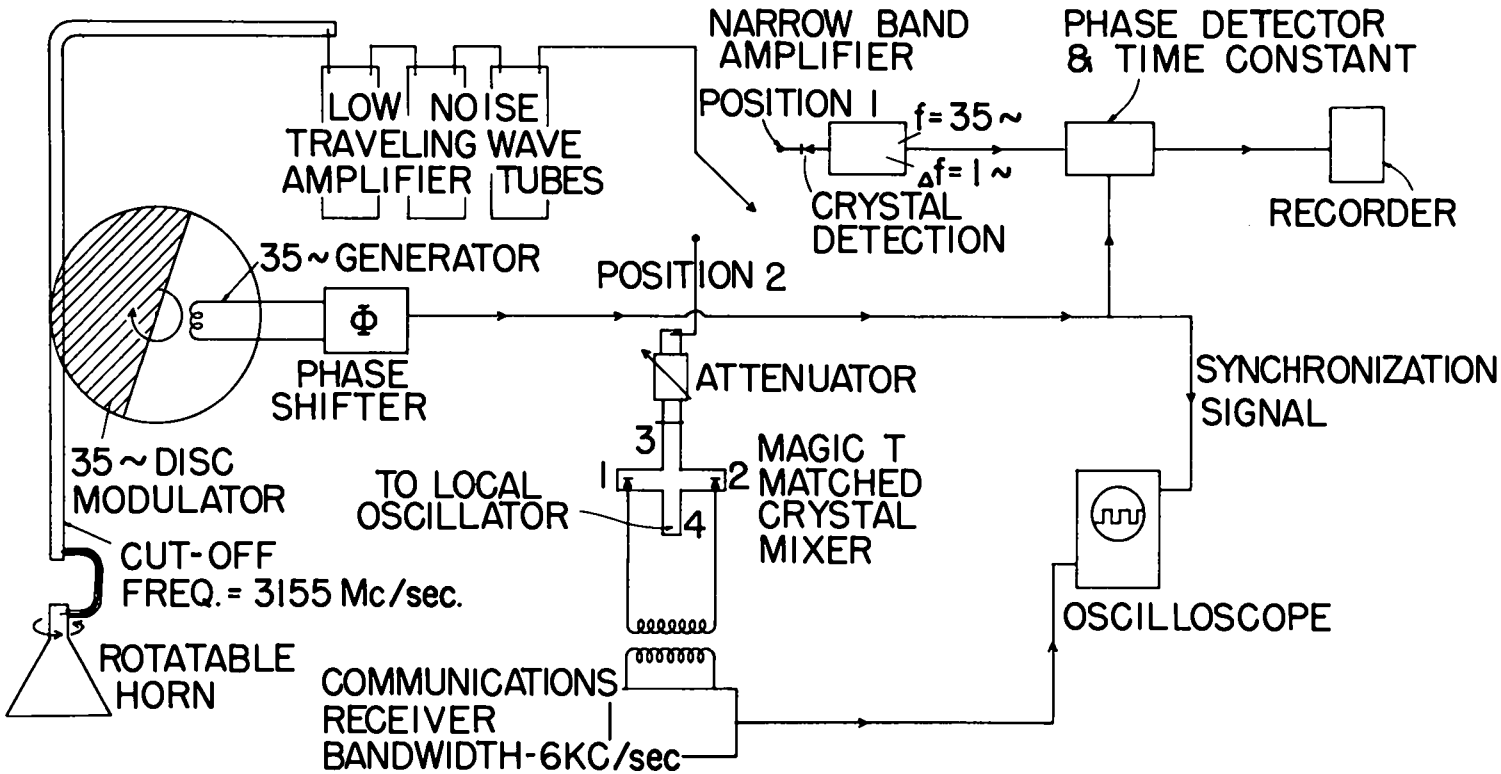


Fig. 9. Schematic of microwave scattering apparatus

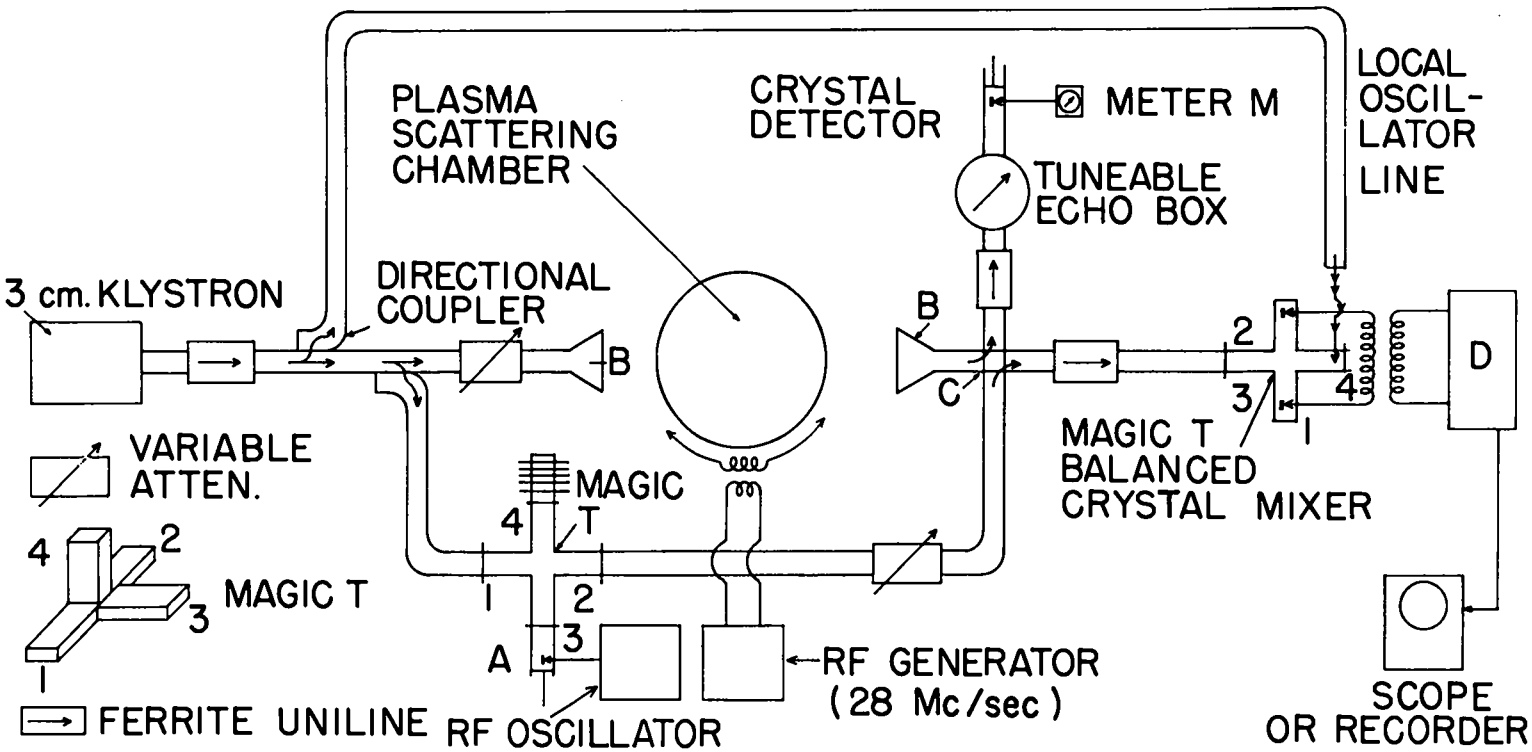


Fig. 10. Schematic of microwave scattering apparatus

borders on the carrier. The gas is ionized by means of two thin copper rings strapped to the Pyrex chamber (Fig. 7), and coupled to a 1-kw Johnson RF transmitter operated at 28 Mc/sec. Average electron density in the center of the chamber is determined by means of a microwave interferometer operated at 10,000 Mc/sec. (See horns B-B in Fig. 6 and see also Fig. 8.)

Radiation scattered incoherently is detected in two ways:

1) A sensitive radiometer (see rotatable horn in Fig. 6 and also Fig. 9) detects radiation scattered at right angles to the high-power primary beam. The input to the radiometer consists of a waveguide whose cut-off frequency exceeds the primary carrier frequency. To date the latter has been fixed at 2600 Mc/sec, and the input cut-off frequency used in these experiments has been 3155 Mc/sec. Preliminary search is carried out with the low-noise (6 to 7 db noise figure) traveling wave tubes whose bandwidth is approximately 1000 Mc/sec. A tuneable communications receiver with a 6 kc/sec bandwidth is used in conjunction with a crystal mixer and local oscillator to narrow the bandwidth when this is desirable.

2) Radiation can also be scattered incoherently in the forward direction. For this purpose, the 10,000 Mc/sec interferometer is modified as shown in Fig. 10. With this arrangement it is possible to detect scattered radiation whose frequency differs from that of the carrier produced by the primary klystron source. A portion of the carrier is transmitted around the plasma and provides local oscillator power for a balanced crystal mixer superheterodyne receiver. Another portion of the carrier is used in the production of artificial side bands. This is accomplished by amplitude modulating a IN23 crystal with a signal derived from a low-power RF generator. The resulting signal consists of the original carrier plus two side bands separated by the frequency of the RF source. One of these sidebands is selected by a tuneable echo box and its amplitude is compared with the carrier transmitted through the scattering chamber. The comparison is carried out at the crystal detector and meter shown in Fig. 10. The amplitudes of sidebands incoherently

scattered by the plasma in the forward directions, and detected by the superheterodyne receiver, are compared with the artificial sidebands. Their amplitudes are equalized by means of the attenuators in the lines. This measurement yields the relative amplitudes of radiation scattered coherently and incoherently in the forward direction. Equipment is being designed to make these comparisons automatically.

With the equipment described,microwaves have been detected which have been incoherently scattered by what are believed to be driven plasma waves. The driving force has been identified with the RF electric fields which maintain the ionized gas in the scattering chamber. The radiation scattered at right angles above 3155 Mc/sec consists of a series of lines which are separated by the frequency (28 Mc/sec) of the Johnson RF ionization generator. Twenty of these lines have been identified so far. This radiation is strongly polarized, and passes through a resonance as the gas pressure (and thus electron density) is changed. Experiments have been carried out in xenon, krypton, neon, helium, hydrogen,and deuterium. With the exception of helium a resonance has been found in each of these gases. The evidence obtained so far indicates that, on resonance, the ratio of electron density to ion mass is approximately constant provided that the RF frequency is held fixed. Under the conditions measured the ion plasma frequency in the central part of the scattering chamber must be approximately 2 Mc/sec. Thus it requires a 200-fold increase in the electron density if the measurements (which involve a frequency of 28 Mc/sec) are to be associated with ion plasma waves. Such densities may exist in the neighborhood of the RF coupling straps; however, attempts to measure the densities have so far failed.

In the forward direction, two sidebands separated by 28 Mc/sec from the carrier have also been detected. Their existence is believed to provide further evidence that the RF fields are driving electron plasma waves. From a measurement of the ratio of sideband to carrier amplitudes it has been deduced that the density fluctuations associated with this

phenomenon correspond to $10^3$ to $10^4$ electrons/cm$^3$. The experiments described above were carried out in the pressure range of 0.1μ Hg 30μ Hg, and the maximum value of the central electron density was measured to be about 2 x $10^{10}$ electrons/cm$^3$.

The primary objective of this work continues to be the detection of radiation scattered incoherently by electron and ion plasma oscillations. To further this goal, high-power equipment in the 10,000 Mc/sec and 35,000 Mc/sec regions is being put into operation.

## H. ORTHOGONAL PINCH

Evidence obtained during the past several months shows rather conclusively that azimuthal asymmetries of the axial magnetic field for the orthogonal pinch geometry may reduce the neutron yield by as much as a factor of ~ 3. The field asymmetry was produced either by (a) a bar magnet (field strength ~ 100 gauss) placed along the coil length or (b) by upsetting the normal distribution of the return magnetic flux around the outside of the driving coil. The latter was achieved by bringing into contact with the coil a slab of metal forming a radial fin on the cylindrical driving coil. (The current feedpoint connection is an example of a permanent radial fin.) It is believed that the small field asymmetries produced in either of the above ways affect adversely not only the initial stage of ionization but primarily the uniform detachment of the current layer from the inner surface of the glass wall.

If the Kerr cell photographs taken previously are examined closely, small departures from cylindrical symmetry are observed in the weakly illuminated photographs. The history of these so-called instabilities or radial asymmetries cannot be followed in detail, but they appear not to grow with time as might be expected of a genuine instability. Previous magnetic probe measurements in vacuum have not shown any magnetic field asymmetry greater than 1 percent across the radial plane that contains the feedpoint connection.

Magnetic field damage (100 to 200 kgauss region) in certain azimuthal regions of the brass coil show that the magnetic field adjacent to the feedpoint is larger than at other azimuthal points. Efforts are being devoted to making the cross section of the orthogonal pinch coil highly symmetric except for a small but finite thickness of the feedpoint.

The neutron yield vs voltage has been extended to 22 kv by over-voltaging the capacitors. It was found that the neutron yield increased by a factor ~ 2 per kilovolt increase in the voltage range 15 to 18 kv In the 18 to 22 kv range the neutron yield increased only ~ 1.5 per kilovolt (see Fig. 11). At the higher voltages there is evidence of increased contamination, suggesting that the optimum energy density of the applied electric field for Pyrex glass is being reached.

## I. IRRADIATION OF THE FOUR-ELECTRODE GAPS

Effects of irradiation on the four-electrode Marx gap (Drawing No. 45Y23141) have been studied. A slowly rising trigger pulse, $E_{Trig}$, was applied to the probe of the center electrode. This trigger pulse irradiates the gap and swings the center electrode in the negative direction. Figure 12 is a plot of trigger voltage versus time (measured in units of the time constant to charge up the center electrode) for main gap breakdown. With 20 kv across the main gap, breakdown occurred at ~ 0.25 $E_{Trig}$ and the variation of trigger voltage was negligible. When the main gap voltage was lowered to 2 kv, breakdown occurred between 0.87 and 0.92 $E_{Trig}$. It should be noted that the irradiating current had dropped from 1.32 amp in the 20 kv shots to between 120 and 218 mamp for the 2 kv shots. As the Marx gap is designed to operate up to 30 kv it is possible then to fire the gap from 2 to 30 kv. With a steep trigger pulse the jitter in firing may be kept below 0.1 μsec over this range of main gap voltages.

To check the breakdown point in the unirradiated case the irradiating gap was shorted out with the trigger pulse applied directly to the center electrode with the time constant unchanged. With 20 kv on

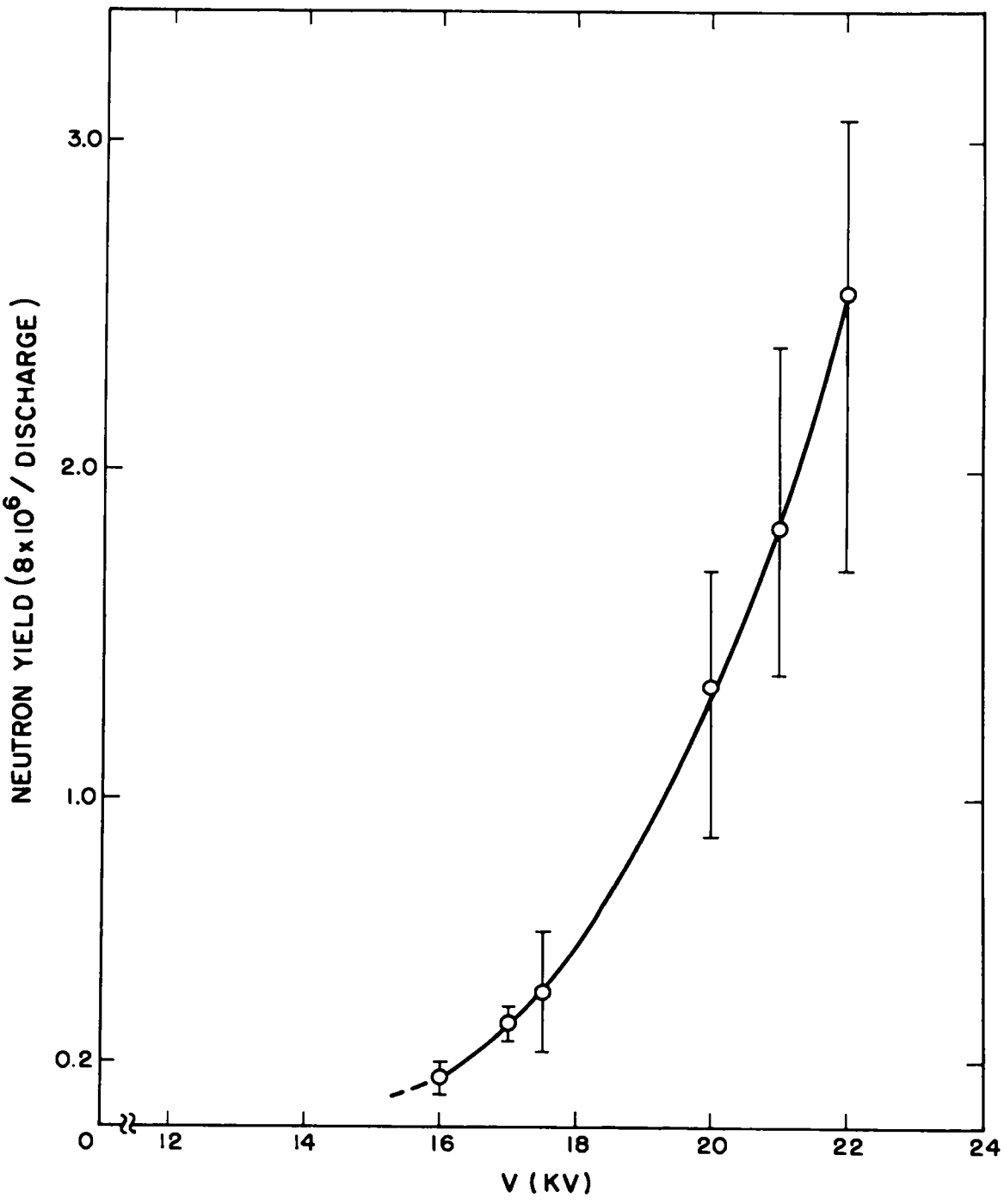


Fig. 11 Effect of voltage on neutron yield in the orthogonal pinch

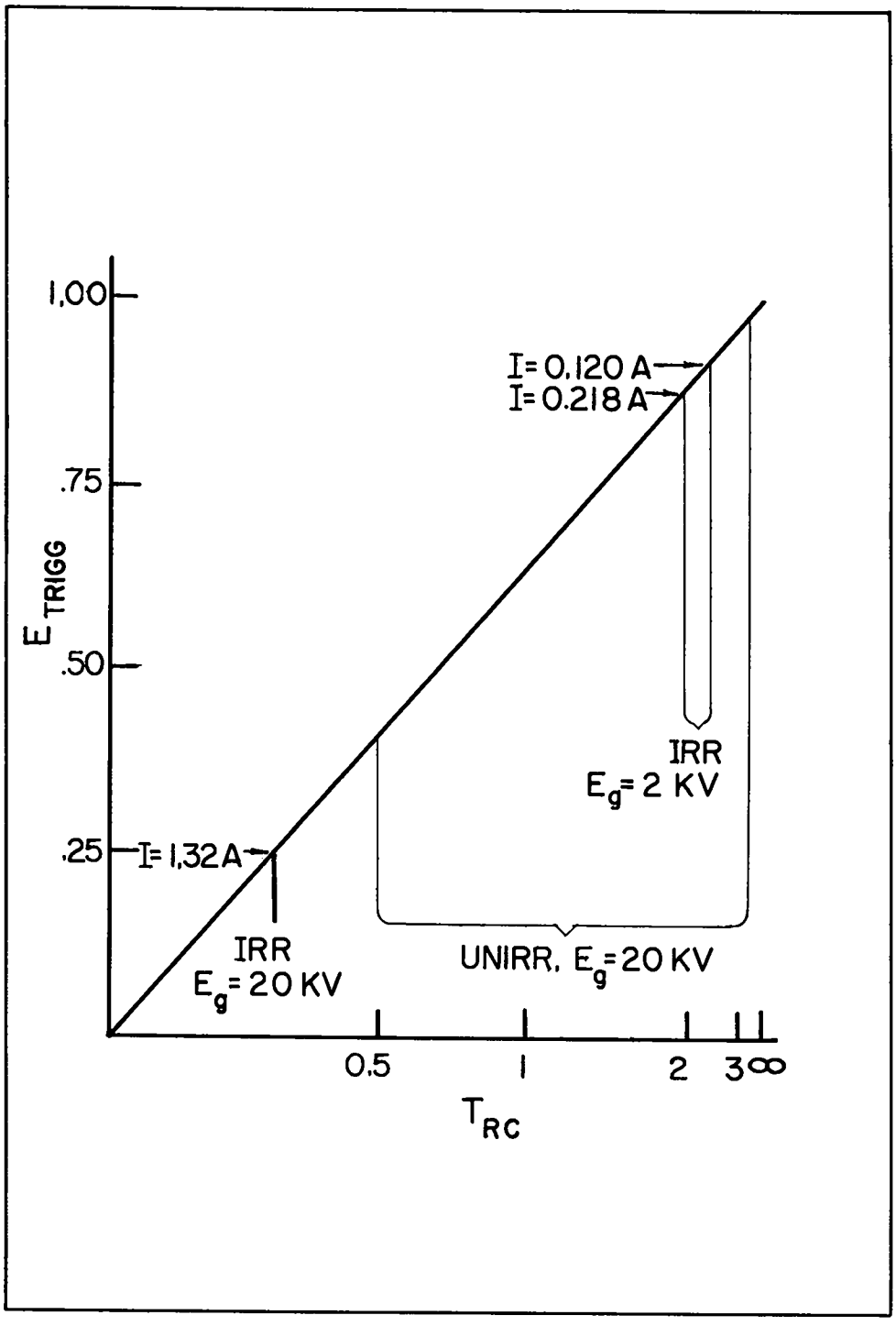


Fig. 12 Trigger voltage versus time (in units of RC) for four-electrode Marx gap

the main gap breakdown occurred between 0.41 and 0.97 $E_{Trig}$ (Fig. 12), and with 19 kv on the main gap breakdown did not occur in two shots out of ten. It is clear that irradiation of the gap reduces the jitter time in firing by orders of magnitude.

With the gap unirradiated but dirty (e.g., oxide coatings formed in the electrodes by previous high-current discharges) the spread in $E_{Trig}$ required for breakdown decreased, probably due to the corona charging up the small dielectric particles on the electrode surfaces.

## J. SCYLLA I SOFT X-RAY MEASUREMENTS

The soft x-ray measurements reported earlier (LAMS-2464, p. 17, LAMS-2488, p. 31) have been continued. Values for the beryl crystal reflectivity have been obtained at five wavelengths corresponding to the characteristic radiations, Cu K, Cu L, Ag L, W M, and Al K. In addition, the discontinuous jumps in the reflectivity due to the absorption edges of the silicon and aluminum crystal constituents were measured, using the continuous spectrum from an x-ray tube. The measured reflectivity R of the beryl crystal is given as a function of the grazing angle in Fig. 13.

The Scylla x-ray spectrum has been measured with no contaminant gases added to the deuterium. Line spectra of O VIII, Na X, and Mg XI are prominent in the discharge, and spectra of Al and Si are weak although the discharge tube is 96% $Al_2O_3$ and the remaining 4% is mostly $SiO_2$ with Na and Mg as trace elements. These results agree qualitatively with previous measurements (LAMS 2488, p. 30) with oxygen contaminant added to the discharge. This interpretation of the line intensities observed is complicated by (a) the relative refractoriness of the constituent wall oxides and hence the composition of the impurities, and (b) the fact that the duration of the discharge is too short to produce steady state populations of the ionic species in the high-temperature, low-pressure discharge.

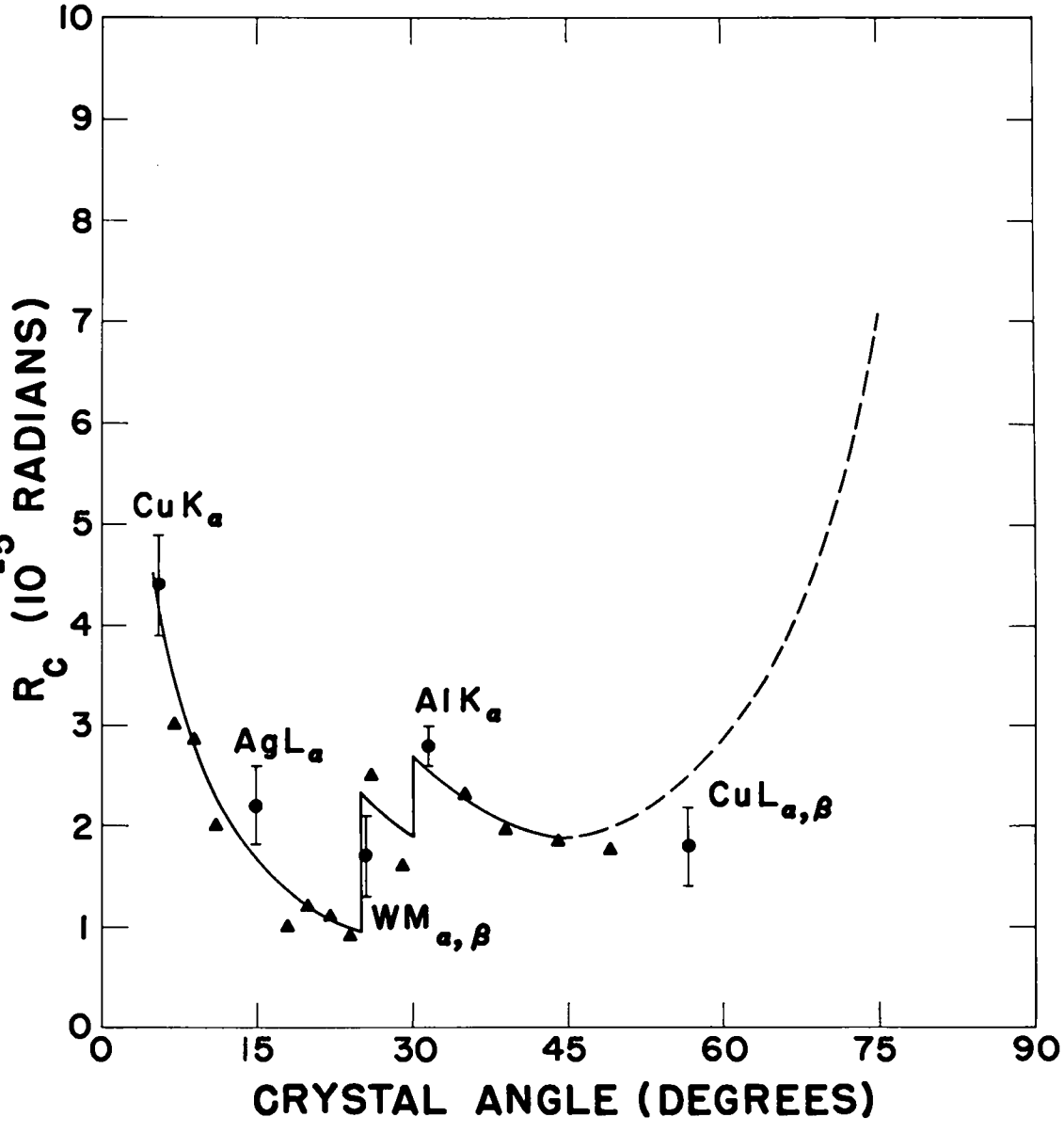


Fig. 13. Reflectivity as function of grazing angle

Observations of the continuum spectrum produced during the second half-cycle of the magnetic compression field are shown in Fig. 14 with line spectra omitted. When plotted as log $dE/d\nu$ vs $\nu$, the continuum should be a straight line of slope $-h/kT_e$, except for quantum mechanical corrections and disturbances due to free-bound continuum limits of impurities. The upper curve in Fig. 14 is for the case of 6% oxygen added to the deuterium gas in Scylla. The lower curve is for pure deuterium gas filling. In both cases, the solid lines are the best-fit theoretical slopes to the experimental points. The electron temperatures derived from these measurements are 295 $\pm$ 25 ev with 6% oxygen and 345 $\pm$ 30 ev for pure deuterium. The greatest uncertainty lies in the experimental measurements of beryl reflectivity as a function of wavelength. The previous analysis of the spectrum by absorption measurements indicated a somewhat lower $kT_e$ (240 $\pm$ 40 ev) because of the contribution of the line spectra produced by discharge contaminants.

The absolute intensity of the continuum emission has also been measured. The x-ray spectrometer was realigned, and the geometry simplified by the removal of the second Soller slit. The collimation introduced by the first slit was compared with calculated values by slit in - slit out measurements with Scylla as the source. The continuum intensity was found to be down by a factor of four from the published value, of which a factor two is due to the influence of lines in the earlier work and the remaining factor of two must be ascribed to slightly different (e.g., different discharge tube) experimental conditions. The continuum intensity is largely due to recombination radiation from the highly stripped impurities in the discharge and is much greater than the radiation to be expected for pure deuterium bremsstrahlung.

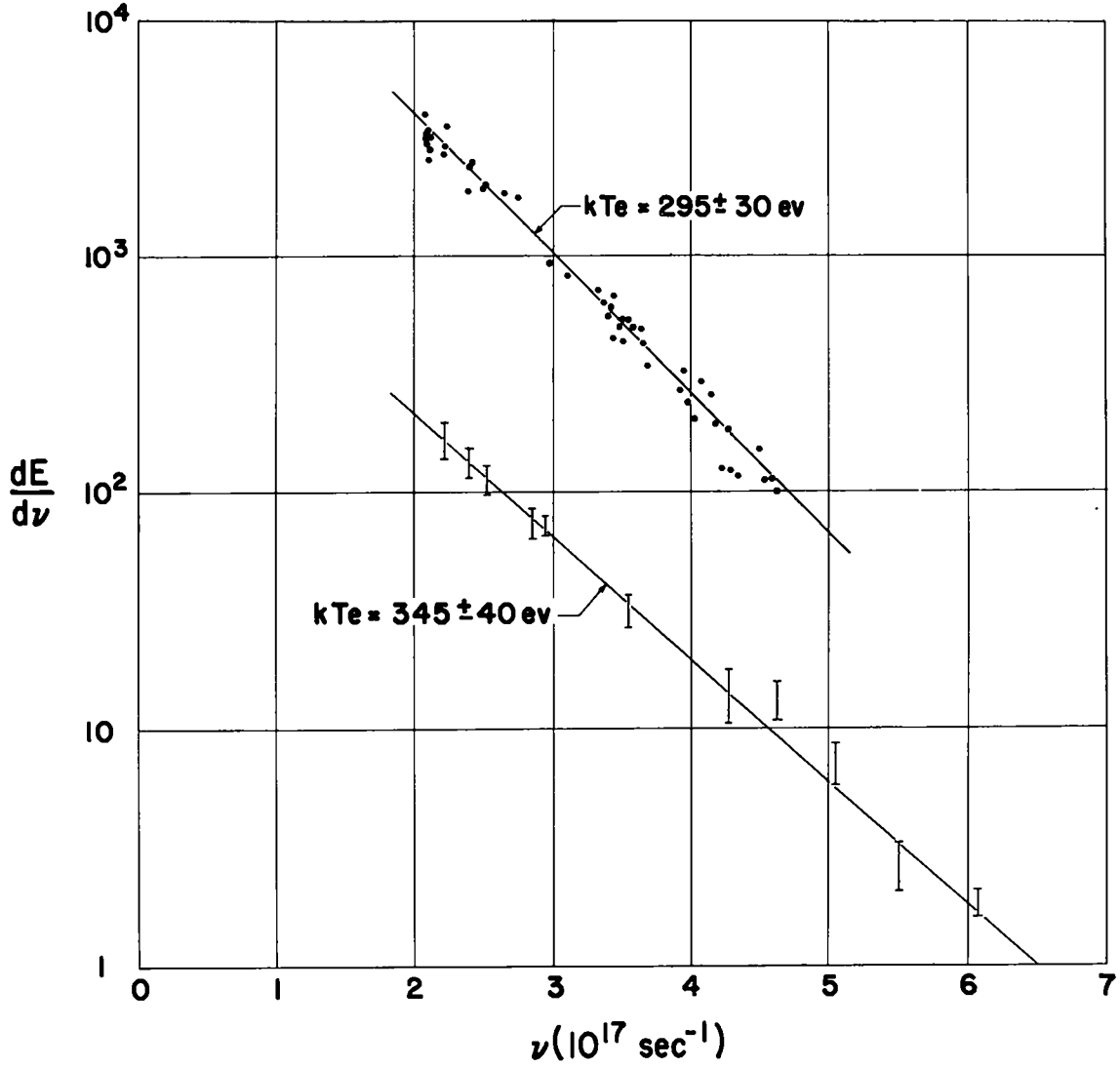


Fig. 14. Continuous spectrum in second half-cycle of Scylla discharge

## K. SCYLLA III

### Neutron Emission and Scaling

Neutron yields as large as $10^8$ per discharge have been observed in Scylla III (LAMS-2488, p. 34), with the "standard" Scylla coil ($\ell$ = 10.6 cm; diam. = 8.1 cm; G.M.R. = 1.4; $L_c$ = 38 mμh). It is of interest to compare this observed yield with the predicted value as determined by scaling the Scylla I results. On the basis of the postulated heating mechanisms, which consist of an initial heating by a rapidly contracting wave to a temperature $T_o$ followed by an adiabatic compression, the following scaling relations are obtained:

From the assumption that the initial temperature $T_o$ is proportional to the initial B in the coil it follows that,

$$\frac{T_{o3}}{T_{o1}} = \frac{\dot{B}_3}{\dot{B}_1} = \left(\frac{\tau_1}{\tau_3}\right)^2 \frac{K_3}{K_1} ,$$

where $\tau$ is the period of the electrical system, and K is the product of the capacity of the energy storage bank, the charging voltage of the bank, and a geometrical coil factor. On the assumption of an adiabatic compression, the volume compression factor $\alpha$ is given by ($\gamma$ is the specific heat ratio)

$$\alpha = \left( \frac{B^2}{8\pi N_o k T_o} \right)^{1/\gamma} ,$$

where $N_o$ is the initial density and is assumed to be constant. The final temperature at peak compression is

$$T = \alpha^{\gamma-1} T_o .$$

The magnetic fields scale as

$$\frac{B_3}{B_1} = \frac{\tau_1}{\tau_3} \frac{K_3}{K_1} .$$

Therefore,

$$\frac{T_3}{T_1} = \left(\frac{\alpha_3}{\alpha_1}\right)^{\gamma-1} \quad \frac{T_{o3}}{T_{o1}} = \left(\frac{K_3}{K_1}\right)^{\frac{2\gamma-1}{\gamma}} \quad \left(\frac{\tau_1}{\tau_3}\right)^2 ,$$

and the neutron yield scales as,

$$\frac{Y_3}{Y_1} = \frac{\alpha_3}{\alpha_1} \frac{\tau_3}{\tau_1} \frac{\langle\sigma v(T_3)\rangle}{\langle\sigma v(T_1)\rangle} = \left(\frac{K_3}{K_1}\right)^{1/\gamma} \frac{\tau_3}{\tau_1} \frac{\langle\sigma v(T_3)\rangle}{\langle\sigma v(T_1)\rangle} ,$$

where it is assumed that the neutron emission time is proportional to the period of the electrical system.

When Scylla III is scaled from Scylla I with the same magnetic compression coil and voltage the results given in Table I are obtained if $\gamma$ is assumed to be 5/3.

TABLE I

| | Scylla I | Scylla III | Scylla III' | Scylla III'' |
|---|---|---|---|---|
| C | 8.7 μf | 26.0 μf | 52.0 μf | 78.0 μf |
| $\tau$ | 5.0 μsec | 8.0 μsec | 11.3 μsec | 13.9 μsec |
| T | 1.3 kev | 2.4 kev | 3.0 kev | 3.6 kev |
| Y | $6 \times 10^6$ | $2.6 \times 10^8$ | $1.4 \times 10^9$ | $4.3 \times 10^9$ |

Scylla III with a neutron yield of $10^8$ is within a factor of 2.6 of attaining the predicted yield. If the initial starting temperature $T_{o3}$ does not scale as predicted but is the same as $T_{o1}$ the predicted neutron yield for Scylla III is $1.9 \times 10^8$.

Streak Photography

An NRL model NLC streak camera has been used to photograph the Scylla III discharge. This camera has an f/no. of 2.9 with approximately the same writing speed as the LASL model 104 streak camera (f/4.5),

which was previously used in the Scylla experiments. The improved f/no. of the NIC camera makes it possible to photograph the structure of the Scylla plasma "fireball" during the megnetic compression stage of the discharge; this has not previously been done. The camera has been used to obtain axial photographs of the Scylla III discharge in compression coils with lengths of 10.6 cm, 16.6 cm, and 24.2 cm, energized by 1/3, 2/3, and 3/3, respectively, of the Scylla III capacitor bank.

During the rise of the magnetic field, the central plasma region shows a rapid initial contracting wave with a reflection, which has been observed many times before, followed by a structure which is indicative of a magnetic compression. However, in the vicinity of or after the maximum of the magnetic compression field, what appears to be a rotating structure often develops, with a frequency in the 1 to 5 Mc/sec range. The characteristics of this rotational structure have been studied in the various fractions of the energy available from the Scylla III capacitor bank. The data and results will be presented in a subsequent report.

The time distribution of the neutron emission is asymmetrical in the case of the short 10.6-cm coil, having its maximum before the peak of the magnetic compression field. It becomes quite symmetrical about the field maximum with the 16.6-cm coil. With the 24.2-cm coil the neutron time distributions are either symmetrical or slightly asymmetrical with the peak yield occurring after the maximum of the magnetic field in the latter case. These results with the short coil substantiate an earlier hypothesis that the plasma escapes out of the ends of the coil during the compression phase of the discharge. There also appears to be a correlation between the time distributions of the neutron emission and the rotational structure observed in the streak photographs, particularly in the case of the short coil.

Preionizer

The assembly of a fast, low-energy capacitor bank to preionize the deuterium gas by direct coupling to the Scylla compression coil is nearly completed. With the strong preionization provided by this bank and the addition of suitable bias magnetic fields, it is expected that an "active"

plasma will be produced on the first half-cycle. With a current crowbar applied at the first maximum of the current, it is hoped that it will be possible to use a quartz discharge tube rather than the usual high-alumina ceramic. This will permit visible observation of the plasma transverse to the coil axis. In addition, it will be much easier to obtain discharge tubes which fit the contour of the magnetic mirror coils, which in turn should reduce the wall contamination problem. This preionization approach is probably essential to larger Scylla-type devices.

## L. E X B ACCELERATOR

The construction of the bakeable hydromagnetic (plasma) gun is complete. A vacuum of $7 \times 10^{-5}$ μ Hg has been attained in the gun prior to baking using only a Freon trap above the diffusion pump. The base vacuum of the pump and Freon baffle system alone was $1.5 \times 10^{-5}$ μ Hg. Upon completion of electrical connections and installation of an activated charcoal trap for purifying the deuterium gas, measurements of the gun operation under baked and unbaked conditions will be made. When at least a rough knowledge of the plasma characteristics of the gun is obtained, the E X B portion of the device will be installed.

The gun was fired unbaked and found to have a natural period of 3 μsec. Comparison of this number with the 1.3-μsec period of ignitron switched to Clamshell capacitor arrangement when shorted, shows that 80 percent of the system inductance resides in the gun and its connections. Further gun diagnostic experiments were discontinued for safety reasons, while the electrical hookup of the $B_z$ bank and coil for the E X B accelerator was completed.

Upon activating the coil for the E X B accelerator it was found that excessive movements of the coil structure occurred which would be great enough to break the Pyrex tube which contains the electrodes. The coil has therefore been redesigned.

Parts for the E X B electrode system have been delivered, and the oven for the injection gun has been completed.

## M. PLASMA FLOWING GUIDE FIELD

A coaxial plasma gun, very similar to those constructed before, but cleaned up in certain design features, is being used for studying the entry of a plasma into a magnetic guide field. This work was undertaken as a preliminary to a projected study of the collision of two plasmas. Two colliding plasmas, if they should interact with one another and bring any substantial fraction of the two blobs to rest, would provide a most attractive method of injection with considerable preheating into a thermonuclear reactor. The design of two identical coaxial guns for this experiment is completed and construction will soon start. In the meanwhile the present studies are being pursued.

The plasma ejected from the gun was first introduced into an axial magnetic field coil wound on a glass drift tube 4 ft long and 6 in. in diameter. The motion of the plasma is being studied by its magnetic effects. In the case of a glass tube the plasma interacts electromagnetically with the electric circuit feeding the solenoid in such a way as to increase the current in the solenoid and thus to perturb rather violently the measurements of the diamagnetic effect of the plasma. Accordingly a guide field solenoid has been wound on a stainless steel tube, and magnetic measurements are being made inside. Difficulties have been encountered with currents flowing to the tube wall but these have been overcome with a glass liner inside the stainless steel. The stainless steel tube bearing the $B_z$ winding is 10 in. in diameter, and the glass tube has a diameter of 7 in. Probes have been abandoned as a means of indicating the increase of field caused by compression between the plasma and the flux-conserving stainless steel tube. Instead, insulated wire loops have been cemented at intervals along the glass tube. Each loop encircles the tube, and its integrated emf is a measure of the magnetic flux crowded out by the plasma. Signals are still not reproducible, but they are regular enough to give interpretable results.

With the above arrangement it is possible to measure the increment of energy produced in the guide field region by the introduction of the plasma, making use of pressure balance and flux conservation. In the absence of appreciable amounts of $B_r$, pressure balance requires that

$B_z^2/8\pi + nkT$ should be constant in a single cross-section of the stainless steel tube. This expression, as well as being a measure of pressure, is a measure of the energy density of the transverse degrees of freedom of the plasma together with the magnetic field energy. The outer part of the tube contains no plasma, because of the insulating glass tube, so a measurement of the magnetic field there yields the energy density in the given cross-section. Multiplying this energy density by the cross-section area gives the line density of energy in the tube.

Any increment in the line density of energy is due to the introduction of plasma, but not all of it is plasma energy. Some of it is in increased magnetic field energy caused by the crowding together of the field lines trapped between the plasma and the flux conserving wall. Since the exact extent of the plasma, and the value of $\beta$ inside it are not known, the exact fraction of energy that is in the plasma cannot be calculated and compared with the total energy increment. However, it is possible to make estimates. It turns out that, if a plasma of area a with $\beta = nkT/(nkT + B^2 8\pi)$ is enclosed in a flux tube of area A, the fraction of energy increment is $2 - \beta/(2 - \beta a/A)$. Reasonable values of $\beta$ and a, together with the known value of A, show this fraction to be approximately 70%.

These considerations, together with measured diamagnetic signals, show that the line density of energy increment produced by the plasma moving through the guide field is approximately 3 joules/cm at a distance of 35 cm from the gun muzzle in a guide field of 1800 gauss and with an arbitrarily selected set of gun parameters: hydrogen feed pressure, 45 lb gage; delay after hammer blow first reaches valve, 150 μsec; gun bank, 42 μf at 12.5 kv. This energy persists for about 4 μsec and then begins to fall, reaching zero at approximately 9 μsec. Closer to the gun the energy density is higher and lasts for a shorter time. Farther away it is smaller and persists longer. Apparently the plasma moves fastest at the front with the later parts moving more slowly. Velocities are difficult to determine accurately from the diamagnetic signals except for the velocity of the front

and to some extent, the back, but streak camera photographs show that the velocities of the various parts of the plasma are remarkably constant from shot to shot although the luminescence may vary through wide limits, from one part to another of a single shot as well as from one shot to another. At 35 cm the velocities from one particular shot which appeared typical of all of them were

| Time μsec | Velocity cm/sec |
|---|---|
| 0 | $6.7 \times 10^7$ |
| 1 | $3.6 \times 10^7$ |
| 2 | $2.3 \times 10^7$ |
| 3 | $1.6 \times 10^7$ |
| 4 | $1.3 \times 10^7$ |
| 5 | $1.0 \times 10^7$ |
| 6 | $0.9 \times 10^7$ |

The flux of energy past a particular point in the drift space is the line density of energy multiplied by the velocity. Using the above velocities, the example cited above gives an energy flux at the beginning of the pulse of 187 joules of transverse energy per μsec and a total integrated flux of 360 joules.

One of the interesting questions about the motion of a plasma in a guide field is whether or not transverse energy is conserved as the plasma moves along the field. Energy can be lost either through actual particle loss or through conversion of energy from the transverse to the lengthwise degree of freedom or through cooling by any other mechanism, since there have been indications in the past that gun plasmas contain a large fraction of neutrals. In order to have been accelerated, those neutrals were once ionized, and so there may well be a large amount of recombination which would lead to particle loss. There may also be a transfer of energy from transverse to longitudinal modes, and the plasma would have a tendency to do this since the lengthwise temperature is rapidly reduced by velocity separation, the transverse temperature remaining high. A measurement has

been made to observe such a cooling by the simple expedient of double integration of the loop signals. There is thus obtained a direct measure of the area of the diamagnetic signal vs time. This area is not proportional to energy transfer, but if transverse energy is conserved, and if lengthwise velocity is conserved, and since the energy is roughly linear with the diamagnetic signal, the area should remain constant as measured at various positions along the drift space. Within the accuracy of the measurement ($\pm \sim 10\%$) there is no loss of transverse energy in a 50 cm length of drift along the guide field.

## N. ZEUS

In the program for testing the recently completed sections of the Zeus capacitor bank, 16 of the 42 shelves have been checked out. The others will be tested during the next few months as time permits. The entire bank has been completed except for the installation of the ignitron switches, and this is proceeding as the preliminary tests of the tubes are completed. The tests involve firing the tube at 30 kv and 15 ka for 10 to 20 shots. If a tube does not prefire, or cleans up after prefiring in the first few shots, it is then considered good and is put into the bank. This same test is used to determine if a tube has gone bad in the bank. When prefiring persists on a given shelf, the 16 tubes are removed and run through the Q-Potter. This will usually indicate which tube has been giving trouble.

Assembly and test of one shelf of the bank, using a new low-inductance cabling scheme, has been completed. The present Zeus transmission system uses fuses connected to a parallel plate line. The inductance of a shelf is approximately 0.075 μh. This inductance cannot be significantly decreased using the existing system. Also, the fuses have not shown a high degree of reliability, and there has been some difficulty in holding the transmission lines together during discharge. The new system has three primary advantages. It has a lower inductance, it will protect the bank when a capacitor fails, and it eliminates the parallel plate lines with their associated mechanical problems.

A simplified schematic of the system is shown in Fig. 15. Each capacitor is connected to the switch header with a 22-ft length of RG 17/14 cable. The length was chosen to give a cable inductance of 4.8 times the inductance of the system. This factor is derived by specifying the inductance of the shelf to be 0.1% the system inductance and there are 48 capacitors and cables on each shelf. The inductance of the header assembly is assumed to be negligible.

The header is designed in the shape of a U as indicated in Fig. 16. The capacitor cables connect to the inside of each leg and the load cables to the outside. The design uses the standard ignitron header assembly which is presently installed in Zeus. A di/dt probe is inserted between the two header plates in the connecting link of the U. The load switches and load cables are the same as presently installed on Zeus.

The system protects the bank in case a capacitor fails in the following manner. Assume capacitor number 48 fails while being charged; current from the other 47 capacitors begins to flow into the failed unit. The inductance of the failed capacitor and its cable is essentially 48 times that of the system so the current to the failed capacitor is limited. The current from the first 24 capacitors flows across the detector probe. This probe initiates a pulse which fires the load switches. At this time the good capacitors experience two loads in parallel. The normal load which has 0.9 the system inductance and the shorted capacitor which has at least 4.8 times the system inductance. Most of the energy will go into the normal load. Several runs of this problem on the IBM computer have indicated that the energy dissipated in the shorted capacitor would not be enough to cause it to rupture.

The shelf was connected to a test load which consisted of sixteen 25-ft lengths of type RG 17/14 cable with the ends shorted. The system was fired at voltages up to 5 kv and currents of the order of 450 ka. The load inductance was 0.056 μh and the inductance of the shelf, as determined from the ringing frequency, was 0.030 μh. This is in close agreement with the calculated value.

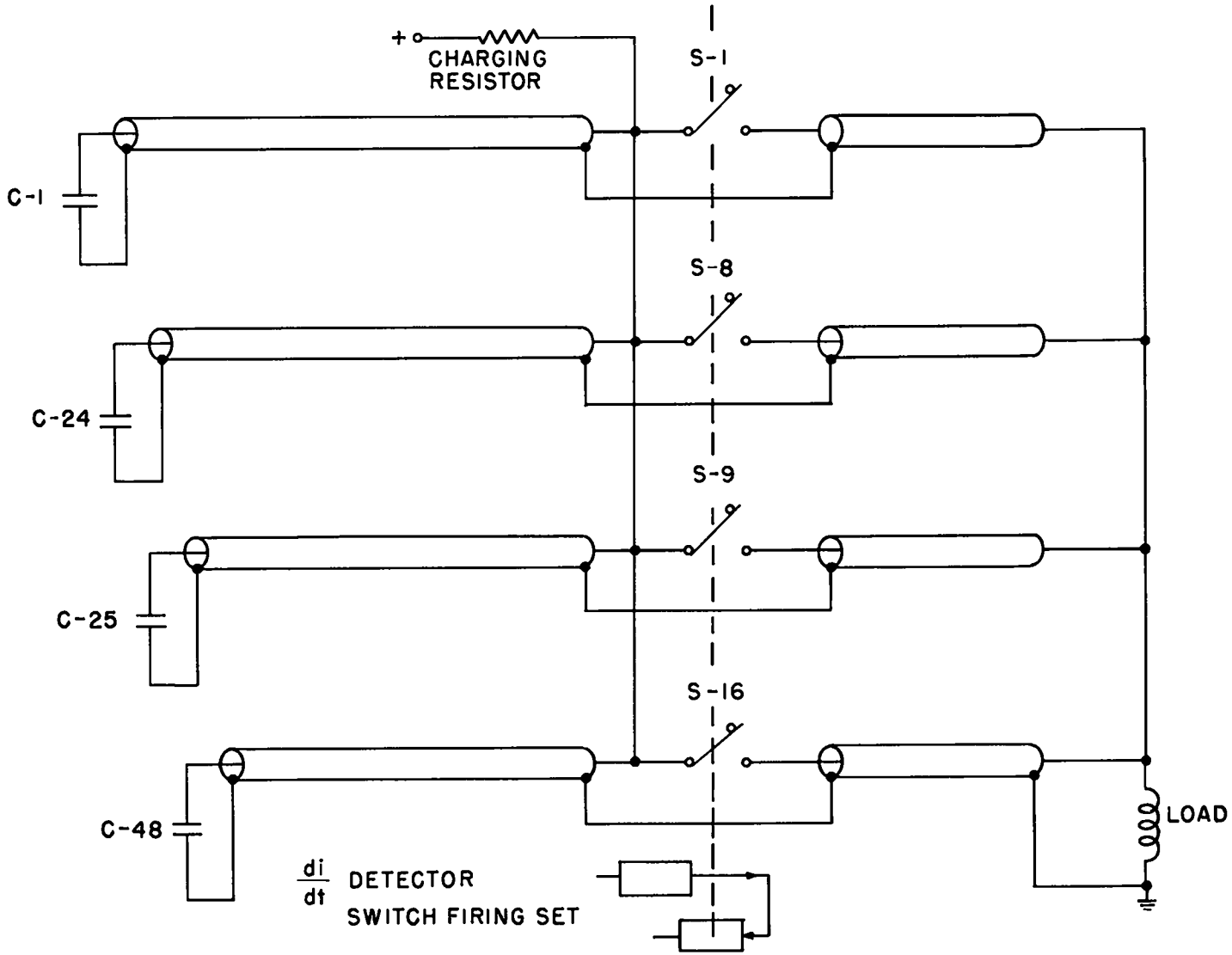


Fig. 15. Schematic of low-inductance cabling scheme for Zeus

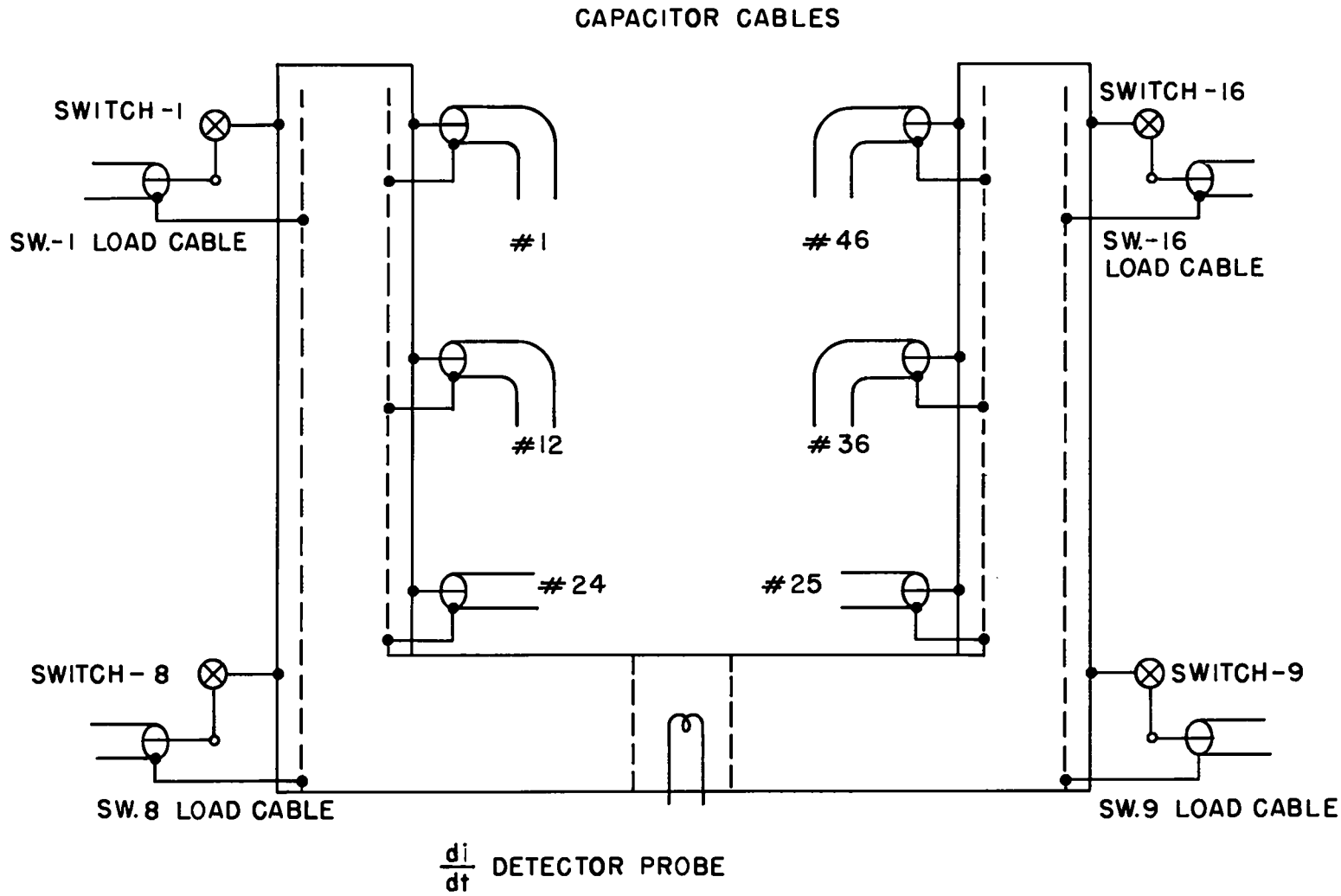


Fig. 16. Schematic of design of header assembly

The protection scheme was also checked at voltages up to 5 kv. The cable from one of the capacitors was disconnected at the header. Another 22-ft cable was substituted, terminated with an ignitron. Firing this ignitron when the capacitors were charged simulated the situation which would occur if a capacitor should short while the bank is charging. The tests showed that the load ignitrons fired 2.7 μsec after the fault was sensed. Analysis of the current wave forms in the system indicated that less than 10% of the total energy went into the short. The shelf stores 140,000 joules at 20 kv. A capacitor can dissipate up to 25,000 joules without serious damage to the can. Thus, the 14,000 joules which would be dissipated in a shorted capacitor under this system can be considered safe.

A further examination of the new header system has indicated several places where some reduction can be made in the inductance. Such changes in the design will be made before any additional header systems are built.

Using the sixteen 25-ft shorted cables as a load, the inductance of shelves on the other racks of Zeus was measured. This load has an inductance (0.056 μh) which approaches that of the shelf and, consequently, gave greater accuracy than had been attained on previous tests. The results are as follows:

| Rack | Shelf inductance (± 5%) |
|---|---|
| 1 | 0.0935 μh |
| 2 and 6 | 0.083 μh |
| 3,4, and 5 | 0.06 μh |
| Cables Shelf | 0.03 μh |

The variation in inductance is caused by the use of different thicknesses of insulation between the parallel plate lines and by modifications which were made in the lines during construction.

## 0. COMPONENT DEVELOPMENT

Development work on the fast parallel-plate capacitor has continued. Effort has been centered on the problem of edge failures. Test samples have been made with two sections (four parallel-plate elements) for evaluation of various design changes. Ten capacitors were made with 30-mil Mylar dielectric and 5-mil copper plates in the same geometry as expected in the finished unit. Tests were run on these samples with dc and with a ringing discharge. All units failed at the edge. The dc failures on five units averaged 46 kv, while on ac test at 2.6 Mc the failures ran between 24 and 35 kv. The tests did show, however, that an adequate design has been found for the tab section so the problems in this area appear to have been eliminated.

Calculations and field plots of the electric field at the edge of the plates have shown that, in the best condition that can be obtained, the field will reach 1.7 times the field between the plates; hence, the corona problem is quite severe. It may ultimately be necessary to change the design in order to use two series sections and thus reduce the voltage per section.

Using similar techniques, an optimum geometry for a voltage gradient element was determined, and test samples are being prepared. Preliminary samples using single voltage gradient elements were run to considerably higher voltages than similar samples without these elements. The field at the edge of the capacitor plate will not be changed under these conditions, but the overall effect of the high field corona may be reduced. By extending the element beyond the edge of the main plates there will be no field concentration on its edge, and therefore a capacitor can be built using voltage gradient elements without increasing the edge effect problem.

It is considered that the present design is suitable for a 30-kv capacitor. A 0.5-μf unit of this design should ring at over 8 Mc and have a Q of the order of 10 to 50 at this frequency. With the modifications outlined above, it is expected that the working voltage can be extended towards 50 kv.